

Gortowski Copy AIR 52032C

PHOTOELASTIC ANALYSIS OF SHEAR STRESS

DISTRIBUTION IN ADHESIVE-BONDED LAP

JOINTS

By

Dieter Kutscha, Chemist

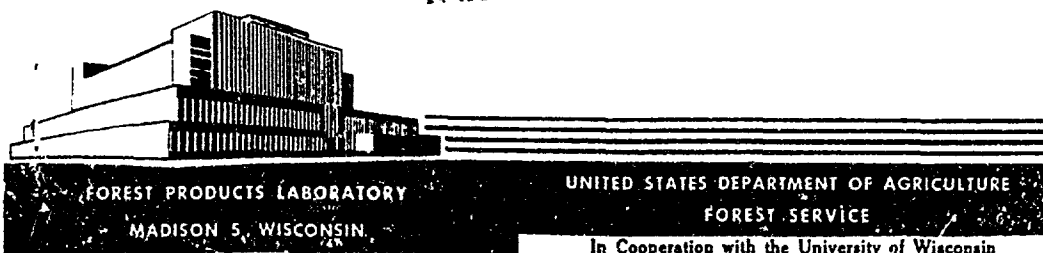
July 1962

TP-122

**BEST
AVAILABLE COPY**

In cooperation with the Bureau of Naval
Weapons, Order No. 19-61-8019-WEPS

DISTRIBUTION OF THIS DOCUMENT
IS UNLIMITED



Gortowski Copy AIR 52032C

PHOTOELASTIC ANALYSIS OF SHEAR STRESS

DISTRIBUTION IN ADHESIVE-BONDED LAP

JOINTS

By

Dieter Kutscha, Chemist

July 1962



AD-640-857

AD640857

CLEARINGHOUSE FOR FEDERAL SCIENTIFIC AND TECHNICAL INFORMATION			
Hardcopy	Microfiche		
\$ 5.60	\$.75	55 pp	as
/ ARCHIVE COPY			

Table of Contents

	<u>Page</u>
Summary	1
Introduction	1
Previous Theoretical Analyses	2
Previous Experimental Studies	6
Photoelastic Stress Analysis	6
Photoelastic Studies	8
Experimental Procedure	10
Preparation of Specimens	10
Instrumentation	11
Testing Procedure	12
Discussion of Photoelastic Analysis	12
Fringe Pattern Development	12
Shear Stress Distribution Along the Lap	13
Shear Stress Distribution with Increasing Load	15
Shear Stress Distribution with Increase in Length of Overlap	15
Shear Stress Distribution Across the Adhesive Film	16
Comparison of Experimental and Theoretical Analyses	17
Conclusions	19
Literature Cited	20

PHOTOELASTIC ANALYSIS OF SHEAR STRESS DISTRIBUTION

IN ADHESIVE-BONDED LAP JOINTS¹

By

DIETER KUTSCHA, Chemist

Forest Products Laboratory,² Forest Service
U.S. Department of Agriculture

Summary

A photoelastic analysis was made of the shear stress distribution in an .064-inch aluminum alloy, adhesive-bonded lap joint. The adhesive that was used was a photoelastic material. The stress distribution was studied directly on the adhesive itself in the joint as a function of increasing load and length of overlap of the adherends. The experimental distribution that was obtained was compared with that predicted by the theoretical analysis of Goland and Reissner.

Introduction

The increasing use of structural adhesives in critical metal and wood assemblies has led to a need for better design methods and procedures for these materials. As with any engineering structure, the proper design of an adhesive joint is based on two factors: (1) A knowledge of the stress distribution in the structure and (2) a knowledge of the mechanical properties of the materials comprising the structure.

The purpose of this report was to investigate a simple lap-type joint by determining experimentally the stress distribution in the joint and comparing it with one of the theoretical analyses that has been developed for simple lap joints.

¹This report deals with research conducted in cooperation with the Bureau of Naval Weapons under BuWeps Order No. 19-61-8019-WEPS.

²Maintained at Madison, Wis., in cooperation with the University of Wisconsin.

Experimentally, the procedure was to make a series of aluminum lap joints with varying length of overlap in which the adhesive film was replaced by a highly photoelastic material. The joint was observed with polarized light passing directly through this adhesive film, parallel to the plane of the joint. Therefore, in effect, the adhesive and photoelastic material were one and the same, and the stress distribution in the adhesive could be studied directly in the adhesive film itself.

The shear stress distribution that was determined experimentally was then compared with that obtained from the theoretical analysis developed by Goland and Reissner (6).³

Previous Theoretical Analyses

A simple lap-type joint is illustrated in figure 1. It is a type of joint that occurs in air-frame construction and, even more important, it is the joint used in all the routine testing of adhesives for metal bonding. As is usual for many empirical routine tests, the lap joint is chosen because it is easy to test and specimens are simple to make, but the test in itself is extremely complex from the standpoint of mechanical behavior. For example, it does not determine a simple mechanical property like the modulus of rigidity of the adhesive but it determines the strength of a structure under a complex stress condition.

As a lap joint is being loaded, the adhesive is initially loaded in pure shear but this is rapidly changed to a condition of shear plus bending. The bending arises because the line of force does not pass through the center of the adherends during the initial load, but instead it is offset by a slight eccentricity at the joint area. Since the joint area is eccentrically loaded, a moment is set up that tends to rotate the joint (fig. 2) until the line of force passes through the center of the adherends. This bending moment changes the stress condition from one of primarily shear stress, in which adhesives have excellent strength, to one of peeling or tensile stress, in which adhesives are not as strong.

The testing of lap joints alone, therefore, will not yield information of the type necessary for the critical design of a structural joint. At most, lap joint testing will provide information concerning the strength of a lap joint with a specific length of overlap, specific adherend thickness, adhesive thickness, specific adherend, and specific adhesive. Should any of these parameters change, it is necessary to test a new set of lap joints.

³Underlined numbers in parentheses refer to Literature Cited at the end of this report.

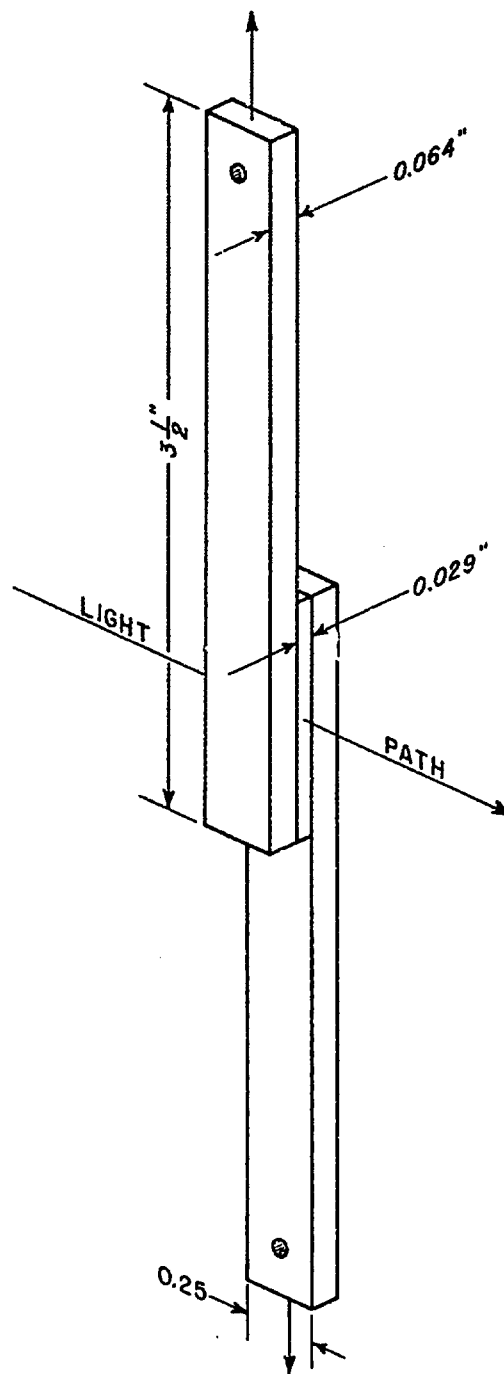


Figure 1.--Illustration of a lap joint showing the direction of load and the light path through the adhesive film.

TP-122

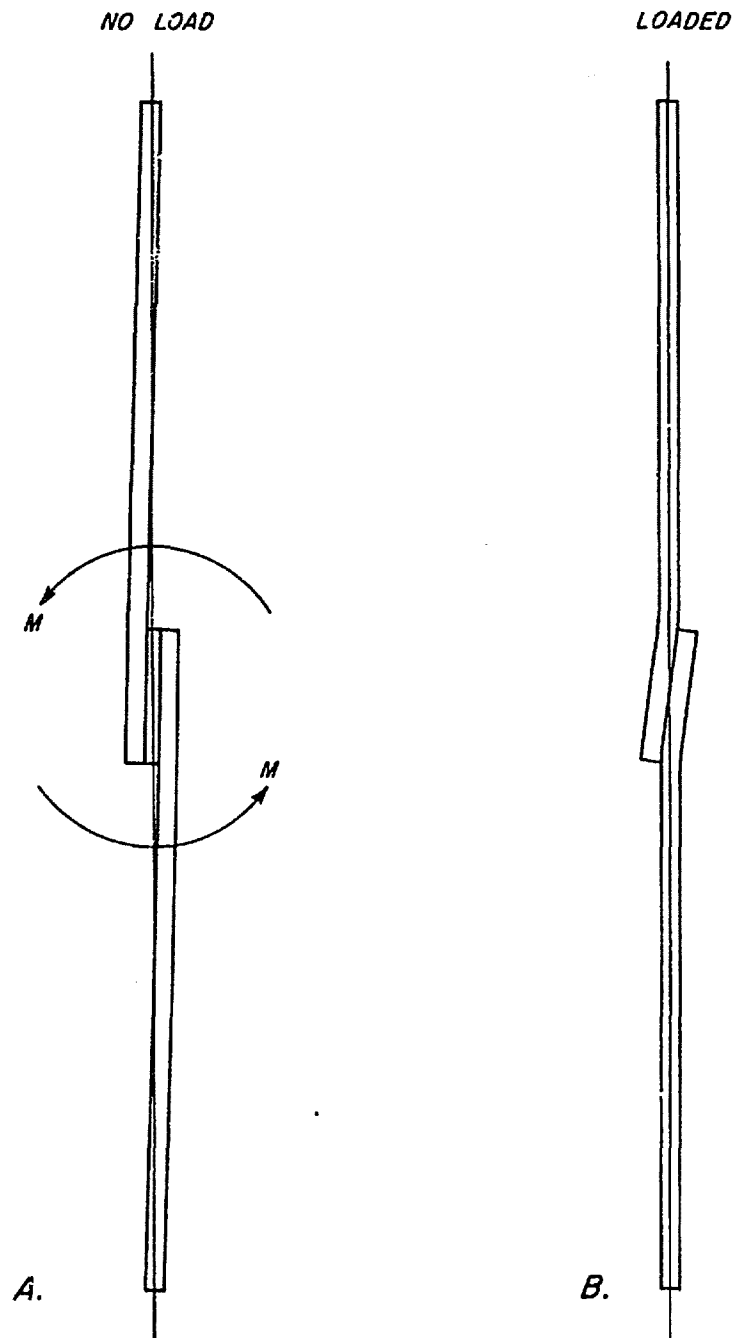
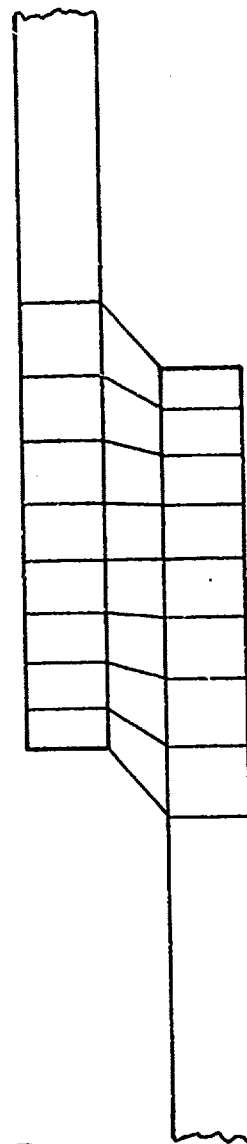
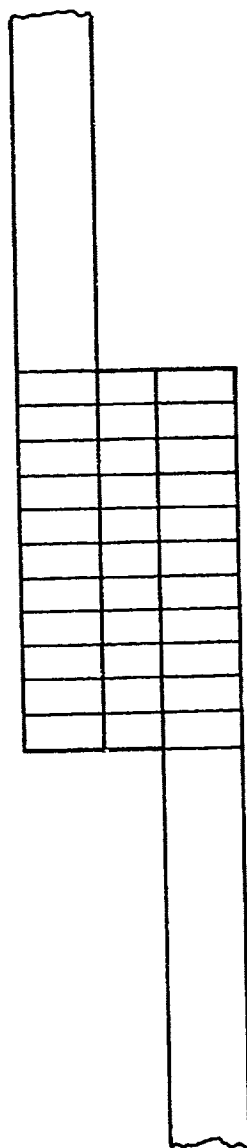


Figure 2. --Bending moment in a lap joint that is due to the eccentric load on the joint area: (A) line of force through the joint before loading; (B) line of force through the joint after loading.

NO LOAD

LOADED



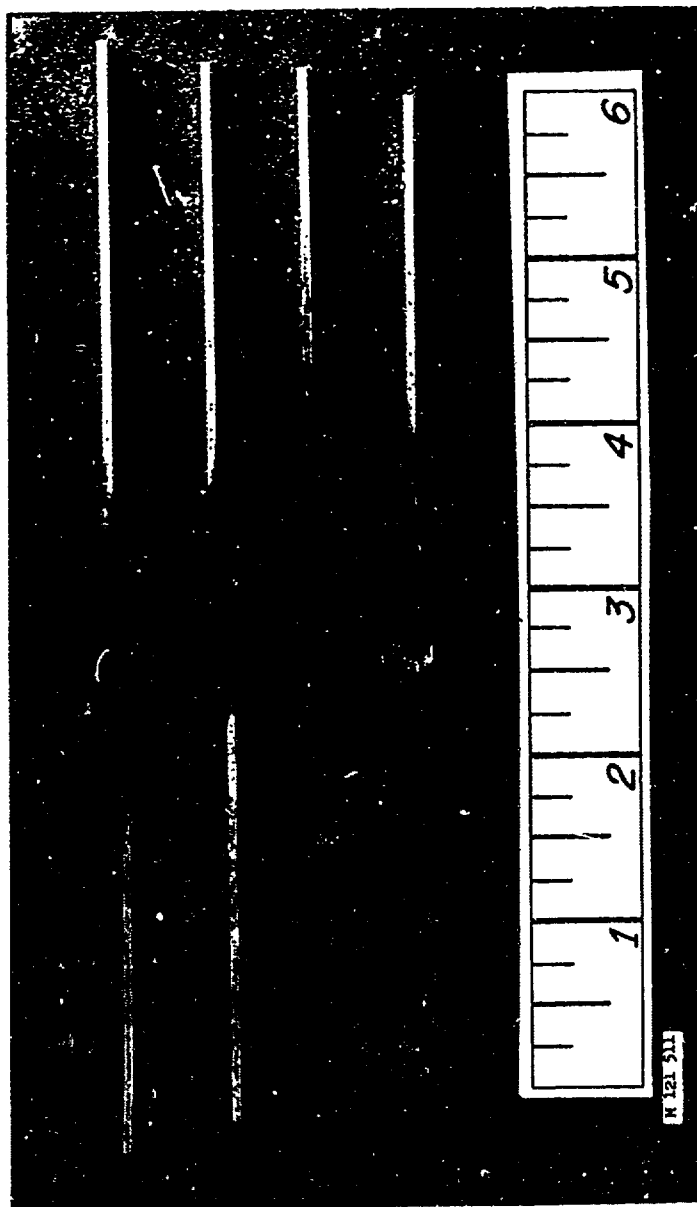
A.

B.

Figure 3. --Differential straining in the lap joint showing the change in a reference grid from (A) before loading to (B) after loading.

Figure 4.--Lap joint specimens used in the study showing the different
lengths of overlap.

(M 121 511)



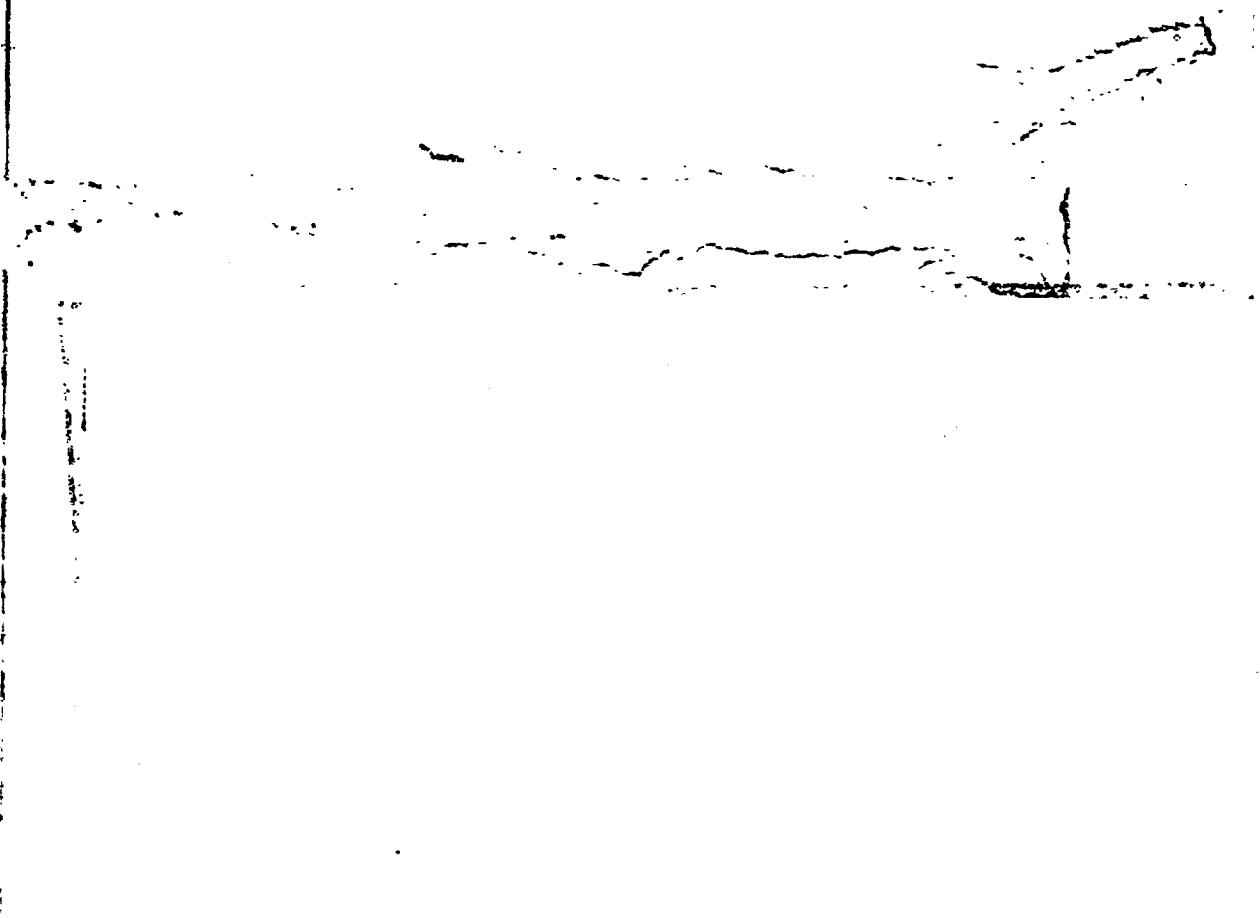


Figure 5.--Experimental apparatus showing (left
to right): the camera, polarizer, loading frame with
dynamometer attached to strain recorder, analyzer,
and light source.

(M 121 381)



Another point to remember is that all the lap-joint testing involves rupture of the joints. This is an ultimate material property that is dependent on statistical variations in such structural inhomogeneities as cracks and internal flaws. These may be entirely unrelated to the chemical nature of the polymer in the adhesive or to the adhesion between the adhesive film and the adherend.

The final point is that lap-joint strengths are based on irreversible processes well beyond the elastic limit. For practical design application, interest is usually in the elastic or, at most, plastic range of behavior where a certain amount of reversible change is expected.

The question arises as to what is the actual stress distribution in the joint. What is the magnitude of the stress concentrations that exist because of the large induced bending moment? Two major analyses of this problem are usually referenced when this subject is under discussion--one by Volkersen (13) and the other by Goland and Riessner (6). Several additional earlier papers (1,4) may be of historical interest to others but these are not discussed here.

If a more complete discussion and wider bibliography of references concerning this area is desired, two readily available references are DeBruyne and Houwink (4) and Benson (2).

Volkersen approached the lap joint problem by simplifying it and considered only the case of a lap joint with differential straining but he ignored bending. Differential straining, as shown in figure 3, arises because adherends are extensible. For one adherend, the tensile strain will be the greatest at the leading edge of the lap and will gradually diminish along the joint, while in the other adherend the highest strain area will be at the opposite end of joint. The result is that the adhesive, acting as the load-transferring member, will suffer the greatest amount of differential straining at the ends of the lap.

Volkersen derived the following relationship for the stress concentration factor (k), the ratio of the maximum shear stress (T_M) to the average shear stress ($T_{av.}$), in a joint with unlike adherends):

$$k = \frac{T_M}{T_{av.}} = \sqrt{\Delta/W} \frac{W - 1 + \cosh \sqrt{\Delta W}}{\sinh \sqrt{\Delta W}} \quad (1)$$

$$\text{where} \quad \Delta = \frac{G_g L^2}{E_2 t_2 t_g} \quad (2)$$

$$W = \frac{E_1 t_1 + E_2 t_2}{E_1 t_1} \quad (3)$$

and

E_1, E_2 = modulus of elasticity of the adherends

t_1, t_2 = thickness of the adherends

G_g = modulus of rigidity of the adhesive

t_g = adhesive film thickness

L = length of overlap

For like adherends, this relationship reduces to

$$k = \sqrt{\Delta/2} \coth \sqrt{\Delta/2} \quad (4)$$

therefore

$$k = f(\Delta) \quad (5)$$

The practice of plotting joint strengths of like materials with varying length of overlap as a function of $\sqrt{s/L}$ (where s is joint strength) is based upon this relationship. It provides a more meaningful relationship for predicting joint strengths than plotting lap shear strength as a function of length of overlap.

The important assumptions of the Volkersen analysis were that no bending took place, the materials were to have Hookean behavior, and the stress across the adhesive film was to be constant.

Goland and Reissner (6) included the effect of specimen bending in their analysis. First, the deformation of the adherends just beyond the joint was determined by the finite deflection theory of cylindrically bent plates, and then the stress distribution in the adhesive in the joint was calculated as a

problem in plane strain. The important assumptions again are that the system behaves elastically and the stress distribution across the adhesive film is constant. For the case of a metal-bonded joint, when the adhesive is relatively flexible compared to the adherends, specifically

$$\frac{t}{G} \leq \frac{1}{10} \frac{t_g}{G_g}$$

The shear stress as a function of joint position is

$$T(x) = \frac{S}{4L} \left[\frac{\beta L}{2t} (1 + 3k) \frac{\cosh \frac{\beta x}{t}}{\sinh \frac{\beta L}{2t}} + 3(1 - k) \right] \quad (6)$$

$$\text{where } k = 1 / \left\{ 1 + 2 \sqrt{2} \tanh \left[\frac{L}{2t} \left(\frac{3\lambda S}{2Et} \right)^{1/2} \right] \right\} \quad (7)$$

$$\beta = \left(\frac{8G_g t}{Et_g} \right)^{1/2} \quad (8)$$

$$\lambda = 1 - \nu^2 \quad (9)$$

and

G = adherend modulus of rigidity

G_g = adhesive modulus of rigidity

t_g = adhesive film thickness

t = adherend thickness

E = adherend modulus of elasticity

ν = Poisson's ratio

S = applied load per inch of joint width

L = length of overlap
 $T(x)$ = shear stress psi at point x
x = position measured from center of joint

Using this function, it is possible to obtain the shear stress at any point in the joint. At the end of the joint, though, the analysis breaks down since the shear stress must go to zero. A shear stress cannot be maintained at a free boundary, and the analysis does not account for this. It is necessary to know the modulus of rigidity of the adhesive also for this analysis.

Previous Experimental Studies

Photoelastic Stress Analysis

The majority of the work that has been concerned with experimentally determining the stress distribution in lap joints has involved photoelastic stress analysis. This technique is based on the study of a transparent material being illuminated with polarized light and viewed through a sheet of polarizing material. If the model or specimen is isotropic, it will not have an effect on the light passing through it, but if the specimen is anisotropic or undergoing strain the polarized light is affected. This change is manifested by the appearance of a series of dark and light fringes if monochromatic light is used for illuminating the specimen or a series of color fringes if white light is used.

Based on the theory of photoelasticity, two types of information can be obtained through an analysis of these fringes.

One set of fringes obtained is known as the isoclinics. These represent the locus of points at which the orientation of the principal stresses is the same. These fringes do not change with increasing load but do change with the relative orientation of the specimen to the planes of polarization of the polarizer and analyzer. The directions of the principal stresses are determined from the isoclinics.

The other set of fringes that appear is known as the isochromatics. These represent the locus of points having a constant value for the difference between the two principal stresses. Since the maximum shear stress at any point in a two-dimensional body is equal to one-half the difference between the principal stresses, the isochromatics represent the locus of points of constant maximum

shear stress. The isochromatics increase in number and change their position in the specimen as the applied load is changed. They do not change as the specimen is rotated relative to the polarizer and analyzer.

Each fringe that appears represents a certain order--the first appearing being number 1, the second number 2, and so forth. If by some method one can identify the fringe order, it can be related to the shear stress by the equation

$$\sigma_1 - \sigma_2 = \frac{f}{h} \times n \quad (10)$$

where n = fringe order

h = thickness of specimen (light path)

f = stress optical coefficient $\frac{\text{lb.}}{\text{in.} \times \text{order}}$

σ_1, σ_2 = principal stresses

The stress optical coefficient is characteristic for any material and represents the stress necessary to produce one fringe in the material.

The isochromatic pattern is analogous to having an infinite number of strain gages on the specimen, and the relative shear stress distribution can be observed by noting the grouping and spacing of the fringes at any point in the specimen.

All the work in this study is based on the analysis of isochromatic fringes; therefore, nothing can be said concerning the directions of the principal stresses in the adhesive.

Hetényi (7) is suggested for a discussion of the field of photoelasticity.

One more important point, which is concerned with the theory of similarity and photoelasticity, needs some comment before reviewing the experimental analyses. Most photoelastic analyses are made on models. For example, if a complex machine part is to be analyzed under a certain load condition, a model of the machine part is made using some type of photoelastic plastic. This model is loaded and analyzed. The very important assumption is then made that the plastic model is "similar" to the machine part and that they both behave the same mechanically.

Because of the experimental difficulty involved in studying small lap joints, the same procedure involving models is used. If models are to be used, the following points should be simulated in the model:

- (1) The discontinuity or interface between the adhesive and adherend.
- (2) The relative ratio of the modulus of the adhesive to that of the adherends. (This is likely to be a low ratio for many joints.)
- (3) The relative ratio of adherend thickness to the adhesive.
- (4) The model should be thick enough in the direction of the light path to assure a condition of plane strain in the adhesive film, which exists in the actual joints.

Photoelastic Studies

Generally, the earlier photoelastic studies involved one of two techniques. One technique was to cut a model out of a single sheet of plastic to resemble a lap joint. Consequently, the adherends and adhesive were of the same material and had the same mechanical properties, but the model had no adhesive-adherend interface. The other technique was to cast or bond a piece of plastic between two metal adherends to simulate the joint, which was the technique used in this study.

The earliest work in this area, though not directly concerned with adhesive joints, was that of Coker (3) on a double shear block. The model was one sheet of cellulose nitrate plastic to which three parallel steel bars were attached making two parallel "glue lines." The two outside bars were pulled in one direction and the center bar was pulled in the opposite direction, thereby creating shear stress in the plastic between the bars. Coker showed that the shear stress is zero at the edge, rises rapidly to a maximum, and then decreases to a minimum in the center of the piece. His model was analogous to a joint with no deformable adherends and a relatively flexible adhesive without bending and, consequently, no tensile stresses (4).

Bollenram (4), using phenol-formaldehyde plastic, and Tylecote (12), using "Xylonite," made similar experiments in which the models were cut with an offset from a single piece of plastic to simulate a lap joint. Their models too, had no adhesive-adherend interface and both adherend and adhesive portions had the same mechanical properties.

The most important work was that of Mylonas (10), who used models in which the adhesive was replaced by a photoelastic material cast in place between

metal or wood adherends. Mylonas' early work involved the study of wide joints with a 0.1-inch-film thickness and a 2-inch overlap. The material he used did not cure uniformly and there was a skin effect. Very high shrinkage stresses were present, and he could not obtain a uniform stress-optical coefficient throughout the model. To overcome the nonhomogeneous adhesive, Mylonas returned to using an offset model cut out of a single sheet of plastic to provide both adhesive film and adherends, but in which the adherend portions were reinforced by stiffening the plastic sheet with steel strips riveted in place. The model looked like an oversized lap joint. With this technique it was possible to study the effect of the shape of the air-adhesive interface on the stress distribution at the end of the joint. The highest stress in the joint occurred at this interface and it was purely tensile.

In later work, Mylonas (11) had greater success with another photoelastic adhesive, and he was able to study further the effect of interface contour on the stress concentration at the interface. For this study, Mylonas used 1/4-inch-thick-aluminum adherends so there is some question whether there was any appreciable bending in the joint area. The adhesive film was as thick as the joint was wide (essentially a block 1/2 by 1/2 inch); therefore, Mylonas points out that this gives rise to a "complex three-dimensional stress distribution caused by the difference of elastic constants of adherends and adhesive and their tendency for unequal lateral strain." So there may not have been a condition of plane strain in the adhesive film. It would be much better to have a larger ratio of width (light path) to film thickness to give a better approximation of an actual joint.

McLaren and MacInnes (9) reexamined the work of Goland and Reissner and extended it to cover a wider range of deformations. They returned to the use of a whole plastic model to simulate adherends and adhesive and also made a composite plastic model by gluing a piece of plastic between two pieces of stiffer plastic to simulate adherends and adhesive.

Based on this brief analysis of the main literature references, it would seem that none of them truly simulated an adhesive joint, judging from the initial criteria for simulation that were proposed. Thus, it was felt another attempt should be made to experimentally approach this problem and try to obtain some data on actual lap joints or at least on joints much more closely approximating an actual joint.

Experimental Procedure

Preparation of Specimens

The specimens that were studied in the present work were a series of aluminum lap joints bonded with Photostress A, a proprietary photoelastic plastic sold by the Budd Instrument Company. The joint variable that was studied was the length of overlap of the aluminum adherends.

Aluminum of 0.064 inch thickness (2024-T3 clad aluminum alloy) was carefully machined into blanks, 3-1/2 by 1/4 inch. The blank surfaces were acetone wiped, vapor degreased, and then etched with sulfuric acid-sodium dichromate solution (5). These blanks were laid up into individual lap joints using shims at the ends of the laps to control the film thickness. The adhesive was allowed to stand for 30 to 40 minutes after mixing in the catalyst before it was applied to the aluminum. This allowed time for the air bubbles to escape, which had been introduced during mixing, and also for the adhesive to increase in viscosity slightly so that it would not run out of the joints. Slight restraint was used to keep the blanks and shims flat while the adhesive precured.

The Photostress A is a 100 percent-reactive material and shrinks only slightly during cure at room temperature. During cure, this plastic reaches a stage where it has sufficient mechanical strength to allow cutting and bending without exhibiting any parasitic birefringence after complete cure. When the joints reach this point, all the excess plastic can be removed with a razor blade, thereby leaving as little material as possible to be removed during final polishing of the specimens.

The ends of the adhesive film were cut perpendicular to the plane of the joint to give a straight, flat air-adhesive interface. The joints were cured for 24 hours at room temperature before final polishing. The edges of the lap joint were polished and cleaned to obtain maximum light transmittance. The polishing was done by hand using abrasive rubber polishers. Kerosene was used to reduce the light scattering from the lightly scratched surfaces when the fringes were being analyzed. Care was taken at all times not to introduce any parasitic birefringence into the specimens. The length of the overlap varied from 0.28 inch to 1.03 inches. The joints that were studied are shown in figure 4. The dimensions of the joints were as follows:

<u>Specimen</u>	<u>Length of overlap (L)</u>	<u>Width or light path (w)</u>	<u>Film thickness (t_g)</u>
<u>No.</u>	<u>In.</u>	<u>In.</u>	<u>In.</u>
T ₂₂	0.35	0.243	0.031
T ₂₃	.28	.231	.029
T ₂₆	1.03	.226	.029
T ₂₇	.75	.221	.029

The ratio of the width of the joint to the film thickness is approximately eight to one, which gives better assurance that a condition of plane strain existed in the adhesive film. If a wider joint (longer light path) than this were used, problems caused by internal reflections from the aluminum adherends would arise.

In order to obtain the lap shear strength of the Photostress Type A, standard 1/2-inch lap shear tests were made with a film thickness of approximately .018 inch. Lap shear strengths varying from 1,290 pounds per square inch to 1,650 pounds per square inch were obtained.

Instrumentation

The basic components of the experimental apparatus were the polariscope, the load frame with the load dynamometer, and the camera (fig. 5).

The polariscope was a standard unit that provided collimated polarized light, either white light or monochromatic light of wavelength 5461 Å. The monochromatic light was generated with a mercury arc and glass filters to isolate the 5461 Å line. The polarizer and analyzer were Polaroid sheet film, and they could both be rotated in their frames.

A small loading frame was built to apply the load to the lap joints (fig. 6). The load was applied by simply turning the nut on either end of the frame. With this frame, the specimen could be easily rotated or moved in the polariscope or the specimen could be loaded and the fringes could be studied while on the stage of a polarizing microscope. This allowed study of the fringes at higher magnifications. The load frame was provided with a load dynamometer consisting of a steel beam mounted on knife edges on which four strain gages connected in an external bridge circuit were mounted. The dynamometer was designed for the load range of 0 to 200 pounds. The maximum stress in the

steel was 20,000 pounds per square inch at the upper limit. The load frame with the dynamometer in place was calibrated in a test machine using an SR-4 strain gage recorder to indicate the strain in the steel beam. The sensitivity of the dynamometer was 1.5 pounds per 10 microinches of deformation of the beam.

The fringe patterns in the specimen were studied either using a stereoscopic microscope for visual observation or a 35-millimeter camera to photographically record the patterns. The camera was a single lens reflex, which made it possible to focus the image by observing the image on the ground glass of the camera.

Testing Procedure

The procedure in loading a specimen was as follows. The specimen was mounted in the frame, and a picture was taken to show the no-load condition. Successive pictures were taken at different increments of load up to usually about 600 pounds per square inch. The load cycle was then reversed, and successive pictures taken coming down in load to show whether any irreversible changes had occurred in the specimens.

To maintain the clarity of the image, it was necessary to keep the specimen surfaces wet with kerosene. The kerosene is not birefringent and has no effect on the fringe pattern other than to make it sharper by reducing the light scatter at the surfaces.

Discussion of Photoelastic Analysis

Fringe Pattern Development

The results of the photoelastic analysis were based on the pictures and photographic slides that were made of the fringe patterns appearing on the specimens. Careful observations were made of the changes that occurred in the fringe distributions as the load was increased so that when the first order fringe had been noted, all the other fringe orders appearing could be identified by simply counting them from the first order. This is not the most accurate method of determining the retardation, but it would have been very difficult experimentally to use some form of compensator with the present apparatus, the very small specimens, and closely spaced fringe patterns. It was felt that by using strain-free specimens at the start and by taking sufficient photographs it would be possible to accurately follow the development of the patterns and accurately identify the fringes.

The general development of the fringe pattern with increasing load for each of the 4 specimens can be seen in figures 7, 8, 9, and 10. The orientation of the specimens in all the photographs was the same. On the left side of each adhesive film the adherend was being pulled up and on the right side the adherend was being pulled down. The photographs show only the adhesive film. The aluminum adherends are not visible since they did not transmit light and because of the lack of contrast between the dark background produced by the crossed polarizer and analyzer and the adherends.

The development of the pattern was the same in all the specimens and it was symmetrical about the center of a properly made joint. The fringes appeared from a source somewhere at the end of the joint. The exact position of this source was not too clear except with specimen T₂₃ (fig. 7, 18). As the load increased, the fringes moved towards the center of the joint. The fringes of like order approached each other from opposite ends of the joint, merged in the center, and then disappeared. The center of the joint represented a sink for the fringes. In all cases, the concentration of fringes was always much higher at the joint ends than at any other point in the joint. From this brief qualitative picture, it can be seen that the ends of the overlap represented the highest stressed areas in the joint and that, when the joint failed, failure would have started at this point.

Shear Stress Distribution Along the Lap

The actual quantitative stress distribution in the joint was determined in the following manner. The photographic slides of the fringe patterns were projected onto a large sheet of graph paper with an ordinary slide projector. The coordinates of any fringe were determined relative to the whole joint using a reference grid. When locating a fringe, the center of the fringe was used to determine its position. The fringe position was determined along the upper left hand and lower right hand edge of the adhesive film as they appeared in all the photographs. This corresponded to the fringe distribution along the interface between the adhesive and adherend where the adherends were undergoing the largest amount of bending and the largest amount of elongation that was due to tension. The reason the measurements were taken along these edges, instead of along the center line of the joint or the other edge, was actually arbitrary. This will be discussed further later.

In order to assign a shear stress value to each fringe, the fringe constant (F) had to be known for each joint. These were determined by equation 11:

$$F = f/w \quad (11)$$

where f = stress optical coefficient for Photostress Type A

w = light path, or width of joint

The stress optical coefficient used was 42 pounds per fringe inch, which was obtained from the manufacturers of the Photostress material. This may be high for the joints that were used in this study, which is not too important since the relative shape of the shear stress distribution curves would remain the same even for another value of (f) so that valid comparisons can still be made. The (f) is the same for all the joints because the adhesive for all the joints came from the same batch of material and the joints were cured under the same conditions.

The fringe constants (F) calculated from equation 11 for each joint were as follows:

Specimen	Length of overlap	F
	<u>In.</u>	<u>P.s.i.</u>
T_{23}	0.28	182
T_{22}	.35	173
T_{27}	.75	190
T_{26}	1.03	186

Using the above values, shear stress distributions were obtained for each joint as a function of average shear stress ($T_{av.}$) as shown in figures 11, 12, and 13

where

$$T_{av.} = P/A \quad (12)$$

P = applied load

A = joint area

Shear Stress Distribution with Increasing Load

The effect of increasing load on the shear stress distribution (figs. 11, 12, and 13) is not too clear at first. It would appear that the maximum shear stress at the end of the lap increases quite rapidly compared to that at the center of the joint as the load increases. This was not the case. The stress concentration factor (k) was plotted as a function of joint position, where

$$k = T_{(x)} / T_{av.} \quad (13)$$

Note that $T_{(x)}$ is the shear stress at (x) , a variable distance measured from the center of the joint. (x) varies from (0) to $(L/2)$ half the length of overlap.

For the 0.35-inch-overlap specimen (fig. 14), the stress concentration distribution is essentially constant with increasing load. There is a slight scatter of the curves, but this is due to the experimental error in determining the original position of the fringes. For the 0.75-inch-overlap specimen (fig. 15), the scatter was greater, especially closer to the center of the joint. For the specimen with an overlap of 1.03 inches (fig. 16), the scatter appears to be even larger at the end of the overlap, and there was also a definite trend in the scatter. The stress concentration at a given point definitely decreased as the load increased. The reason for this may be that the specimen was being stressed beyond the elastic limit in the region at the end of the overlap. A certain amount of plastic flow could have taken place, therefore reducing the maximum shear stress and consequently the stress concentration at that point.

Theoretically, there should be no change in the stress distribution in an elastic material. This is best shown for the 0.35-inch-overlap specimen in figure 14.

Shear Stress Distribution with Increase in Length of Overlap

The effect of changing the length of overlap on the shear stress distribution in a joint can be qualitatively seen by a comparison of figures 14, 15, and 16. For each joint a curve represented one average shear stress that was common for all three specimens. Figure 14 has a curve for 370 pounds per square inch, figure 15 a curve for 380 pounds per square inch, and figure 16 a curve for 395 pounds per square inch. These three curves are combined in figure 17.

Although there was a maximum difference of 25 pounds per square inch, this was not significant for a qualitative comparison.

There was a very definite increase in the maximum stress concentration in the joint as the length of overlap increased. Figure 17 very graphically illustrates why the strength of a lap joint is not increased by increasing the length of overlap beyond some initial length of overlap. At any average shear stress in the lap joint with an overlap of 1.03 inches, the maximum shear stress is about 3.5 times the average shear stress, while, in the 0.35-inch joint, the maximum shear stress is only 1.75 times the average shear; therefore, the larger lap joint will reach the failing load in shear before the smaller lap joint.

Shear Stress Distribution Across the Adhesive Film

One of the basic assumptions common in the theoretical analyses was that the stress distribution across the adhesive film from one adherend to the other is uniform. This was not true as is illustrated by the 0.28-inch lap joint (fig. 18). If the shear stress was constant across the adhesive, the fringes would appear as lines perpendicular to the line of the joint lying across the adhesive film. In figure 18 and in the other photographs, the fringes were almost never straight and never perpendicular to the line of the joint. They were always curvilinear, lying at an angle to the joint.

From a study of figure 18 and the other photographs, it appeared that the fringes were generated from a point on the adhesive-air interface in the form of ellipses. As the ellipse increased in size, it passed off the edge of the adhesive. The fringe pattern on the joint, consequently, represents a narrow band through the pattern of eccentric ellipses (fig. 19).

The lowest order fringe will be the furthest from the common point on the interface since the fringes were observed to move away from this point with increasing load. For discussion purposes let this fringe be labeled as the first order, and the other fringes labeled accordingly. The shear stress does fall to zero at the very end of the joint, as it should theoretically. On the actual joints, this is difficult to see since the fringes are crowded extremely close together at this point. Where the fringe order is plotted across the joint at line (a), it measures from zero up to four plus and then returns back to zero. It is evident that the stress distribution across the joint is not constant.

Comparison of Experimental and Theoretical Analyses

One of the primary objectives of this study was to compare the shear stress distribution obtained experimentally to that predicted by a theoretical analysis, specifically the analysis made by Goland and Reissner. The equation that was used was No. 6 given earlier in the review of previous work. To use this equation, the modulus of rigidity (G_g) of the adhesive was needed, which was calculated from values given for the modulus of elasticity ($E_g = 420,000$) and Poisson's ratio ($\nu' = .36$) using equation 14. These values were obtained from the manufacturers of the Photostress material.

$$G_g = \frac{E_g}{2(1 + \nu')} \quad (14)$$

$$G_g = 155,000 \text{ p.s.i.}$$

This equation holds true only for an isotropic material and there may be some question as to whether the adhesive cured in place in a joint is completely isotropic.

The restriction on the Goland and Reissner equation is that

$$\frac{t}{G} \leq \frac{1}{10} \frac{t_g}{G_g} \quad (15)$$

where $G = 486,000$ is the modulus of rigidity of the aluminum as determined by Kuenzi (8). A check of this for the joints in this study gave

$$\frac{0.064}{486,000} \leq \frac{0.029}{155,000} \quad (16)$$

or

$$1.3 \times 10^{-7} \leq 1.8 \times 10^{-7} \quad (17)$$

Therefore, the restriction was satisfied.

To simplify the work in calculating the shear stress distribution, the Goland and Reissner equation was programmed in Fortran for an IBM 1620 digital computer. An example of the calculated stress distributions that were obtained as the average shear stress changes is shown in figure 20 for the 0.35-inch-overlap specimen.

Comparisons of the theoretical and experimental stress distributions were made at one average shear stress for each of the lengths of overlap--0.35 inch, 0.75 inch, and 1.03 inches. These data are shown in figures 21, 22, and 23. In none of the cases did both analyses give the same result. Generally, the experimental shear stress was higher than that predicted by theoretical analysis.

For the 0.35-inch overlap (fig. 21), both the general shape of the experimental distribution and its height were different from the theoretical curve. There are several explanations for this. Theoretically, the area under the stress distribution curve must always be the same as that for the average stress distribution, irregardless of the shape of the distribution. The area under the experimental curve was planimeted and found to be larger than the area under the average stress curve. This would indicate that the fringe constant for the specimen was too large. If the fringe constant were smaller, the area under the curve would decrease. The true fringe constant could be determined by matching the areas under the experimental and average stress curves. The area under the theoretical curve was closer to what it should be. Some difficulty is introduced in the determination of these areas since the actual shape of the curve at the end of the overlap where the shear stress falls to zero is not known.

From a comparison of the shape of experimental and theoretical curves it would appear that the value used for the modulus of rigidity of the adhesive was too low, as much as a factor of one-half too low. The reason was that, as the modulus of rigidity of the adhesive increases, the slope of the shear distribution increases markedly. This is shown in figure 24 where the shear distribution was calculated as a function of modulus of rigidity of the adhesive at an average shear stress of 686 pounds per square inch for 0.35 inch overlap, for a G of 155,000 and then, arbitrarily, 250,000 and 350,000. The shape of the curve at 350,000 pounds per square inch shear modulus did give a better fit to the experimental curve. This would indicate that in bulk form, the Photostress material had a modulus of 155,000, but in a small adhesive film, its modulus was closer to 350,000.

For the 0.75-inch-overlap specimen (fig. 22), there appeared to be better agreement between the experimental and theoretical curves. The shape and magnitude of the distribution agrees well near the center of the lap but then the slope of the theoretical curve decreases toward the end of the lap.

For the specimen with an overlap of 1.03 inches, the magnitudes of the curves are both different. The shapes of the two curves compared quite well. Although the theoretical curve should be slightly steeper at the end of the overlap, these two curves appear to differ by an increment of load. This can be seen by comparing figure 23 with figure 13.

In the discussion above, the assumption is made that the Goland and Reissner analysis is a good theoretical model for explaining lap-joint behavior. If this is not true, then it can generally be said that this analysis gives values for shear stress lower than those actually occurring.

Conclusions

The experimental technique of photoelastic stress analysis has been satisfactorily applied to study the shear stress distribution in an actual adhesive-bonded lap joint. The technique of using a photoelastic material as the adhesive in a joint could be used to study other joints of more complex geometry.

The study showed that the shear stress concentration distribution in a lap joint remains constant with increasing load and that it increases with an increase in the length of overlap. It was shown that the shear stress across the adhesive film is not constant.

The question of whether the Goland and Reissner analysis accurately describes the shear stress distribution has not been completely answered. Some more careful work is necessary to determine the actual modulus of rigidity of an adhesive in a joint and also to determine the stress-optical constant for material in such a small specimen. Generally, it would appear that the theoretical analysis is low in its prediction of shear stress.

Literature Cited

- (1) Arnovlečić, I.
1909. Das Verteilungsgesetz der Haftspannung bei axial beanspruchten Verbundstäben. Zeitschrift für Architektur und Ingenieurwesen, Hannover, 2: 414-418.
- (2) Benson, N. K.
1961. The Mechanics of Adhesive Bonding. Applied Mechanics Reviews, 14(2): 83-87.
- (3) Coker, E. G.
1912. An Optical Determination of the Variation of Stress in a Thin Rectangular Plate Subjected to Shear. Proceedings Royal Society (London), 86(A587): 291-319.
- (4) DeBruyne, N. A., and Houwink, R.
1951. Adhesion and Adhesives. Elsevier Publishing Company, New York, 91-143.
- (5) Eickner, H. W., and Schowalter, W. E.
1956. A Study of Methods for Preparing Clad 24S-T3 Aluminum Alloy Sheet Surfaces for Adhesive Bonding. Forest Products Lab. Rept. No. 1813.
- (6) Goland, M., and Reissner, E.
1944. Stresses in Cemented Joints. Journal Applied Mechanics, 11(1): A17-A27.
- (7) Hetényi, M.
1950. Handbook of Experimental Stress Analysis. John Wiley and Sons, New York, 828-976.
- (8) Kuenzi, E. W.
1956. Determination of Mechanical Properties of Adhesives for Use in the Design of Bonded Joints. Forest Products Lab. Rept. No. 1851.
- (9) McLaren, A.S., and MacInnes, J.
1958. The Influence on the Stress Distribution in an Adhesive Lap Joint of Bending of the Adhering Sheets. British Journal of Applied Physics, 9: 72-77.
- (10) Mylonas, C.
1948. On the Stress Distribution in Glued Joints. Proceedings 8th International Congress of Applied Mechanics, London, 137-149.

(11) Mylonas, C.

1954. Experiments on Composite Models with Application to Cemented Joints. Proceedings Society Experimental Stress Analysis, 12: 129.

(12) Tylecote, R. F.

1941. Spot Welding. Welding Journal 20: 359s-368s.

(13) Volkersen, O.

1938. Die Nietkraftverteilung in Zugbeanspruchten Nietverbindungen mit Konstanten Laschenquerschnitten. Luftfahrtforschung, 15: 41-47.

Figure 6.--Loading frame with a specimen in place and the beam dynamometer
attached to the strain recorder.

(M 121 510)

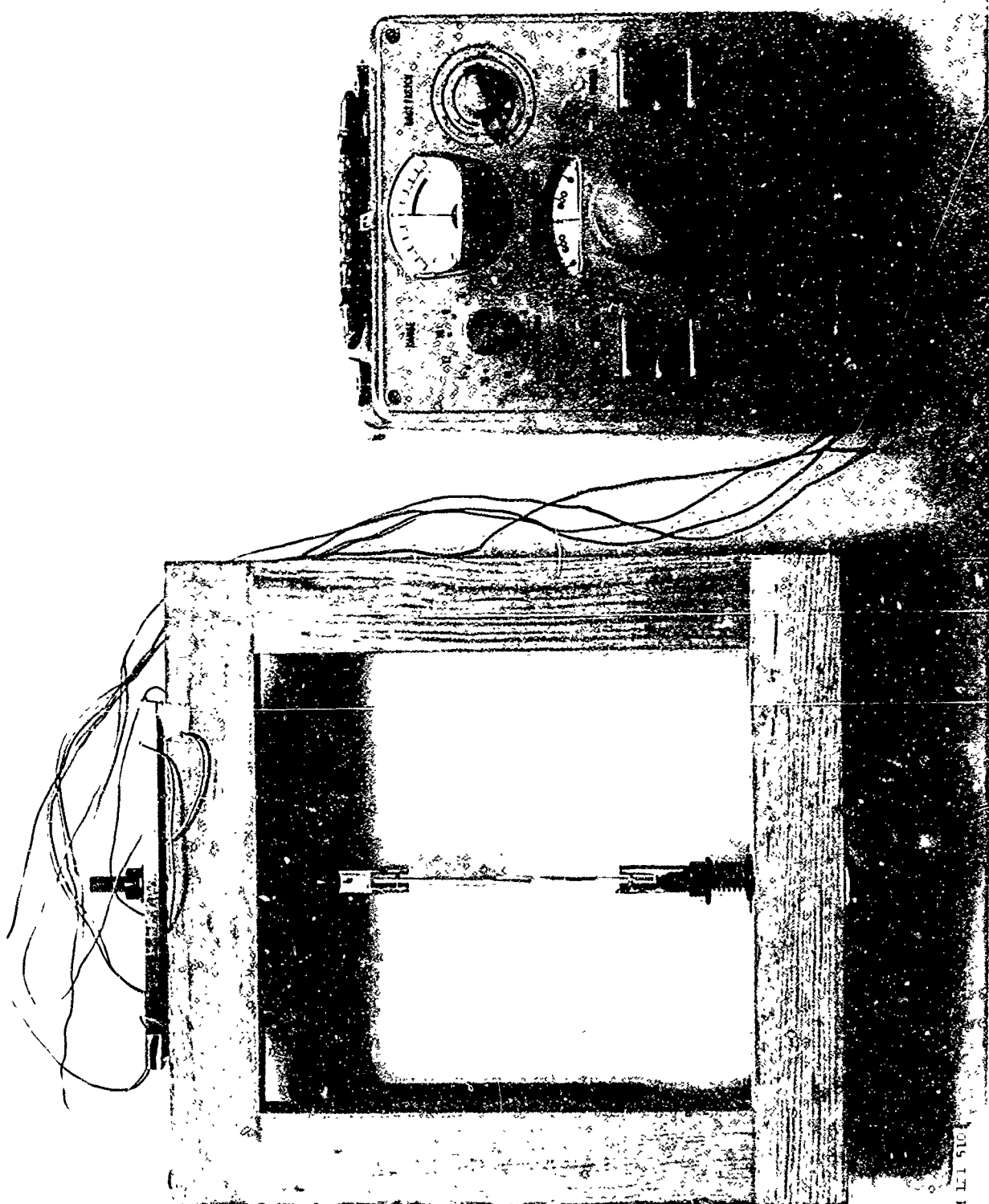


Figure 7. --Fringe pattern development in the adhesive
film of the specimen that had a 0.28-inch overlap.
The average shear stress at the time of exposure is
shown for each frame.

(M 121 557)



243 PSI



382 PSI



J 475 PSI



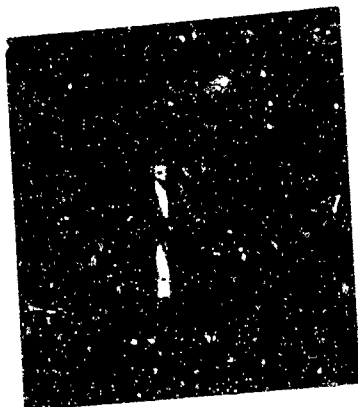
545 PSI



580 PSI



684 PSI



730 PSI

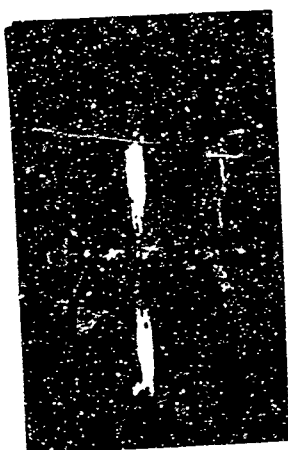
M 121 557

Figure 8.--Fringe pattern development in the adhesive film of the specimen that had a 0.35-inch overlap. The average shear stress at the time of exposure is shown for each frame.

(M 121 558)



158 PSI



216 PSI



317 PSI



370 PSI



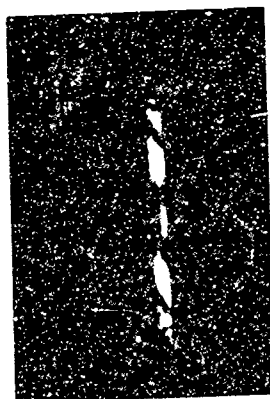
423 PSI



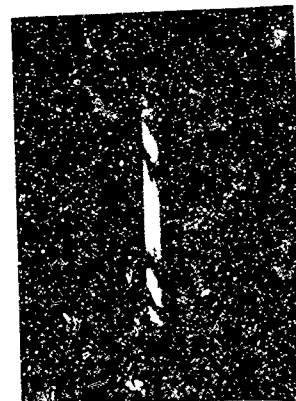
475 PSI



528 PSI



582 PSI



686 PSI

Figure 9.--Fringe pattern development in the adhesive
film of the specimen that had a 0.75-inch overlap.

The average shear stress at the time of exposure is
shown for each frame.

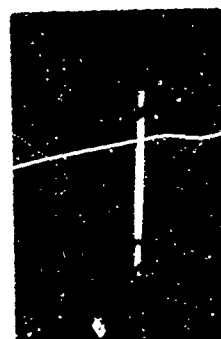
(M 121 555)



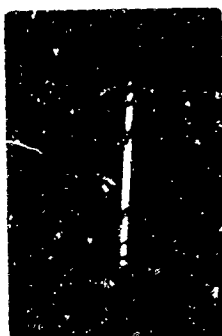
22.6 PSI



85.9 PSI



173 PSI



285 PSI



343 PSI

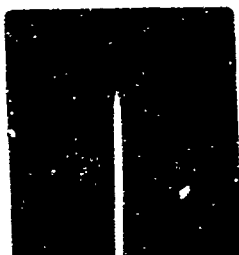


390 PSI

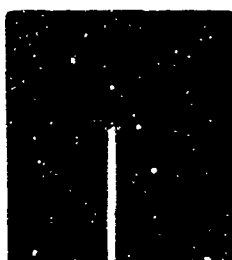
M 121 555

Figure 10.--Fringe pattern development in the adhesive film of the specimen that had an overlap of 1.03 inches. Only one half of the specimen was visible in this series. The average shear stress at the time of exposure is shown for each frame.

(M 121 556)



• 29 PSI



71 PSI



190 PSI .

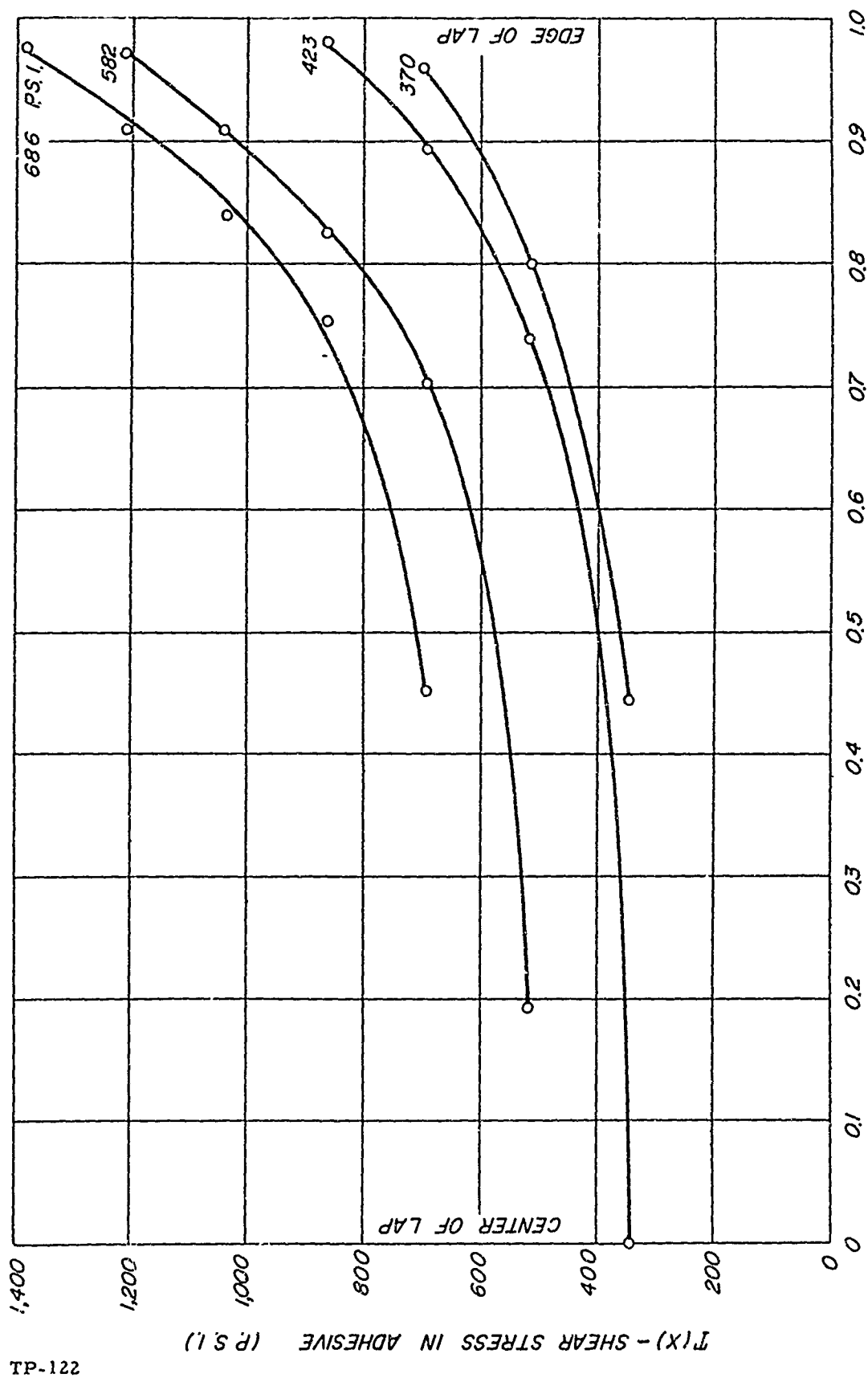


215 PSI



383 PSI

M 121 556



X/L - RELATIVE JOINT POSITION

Figure 11.--Shear stress distribution as a function of average shear stress that was experimentally determined for the specimen that had a 0.35-inch overlap. $l = L/2$

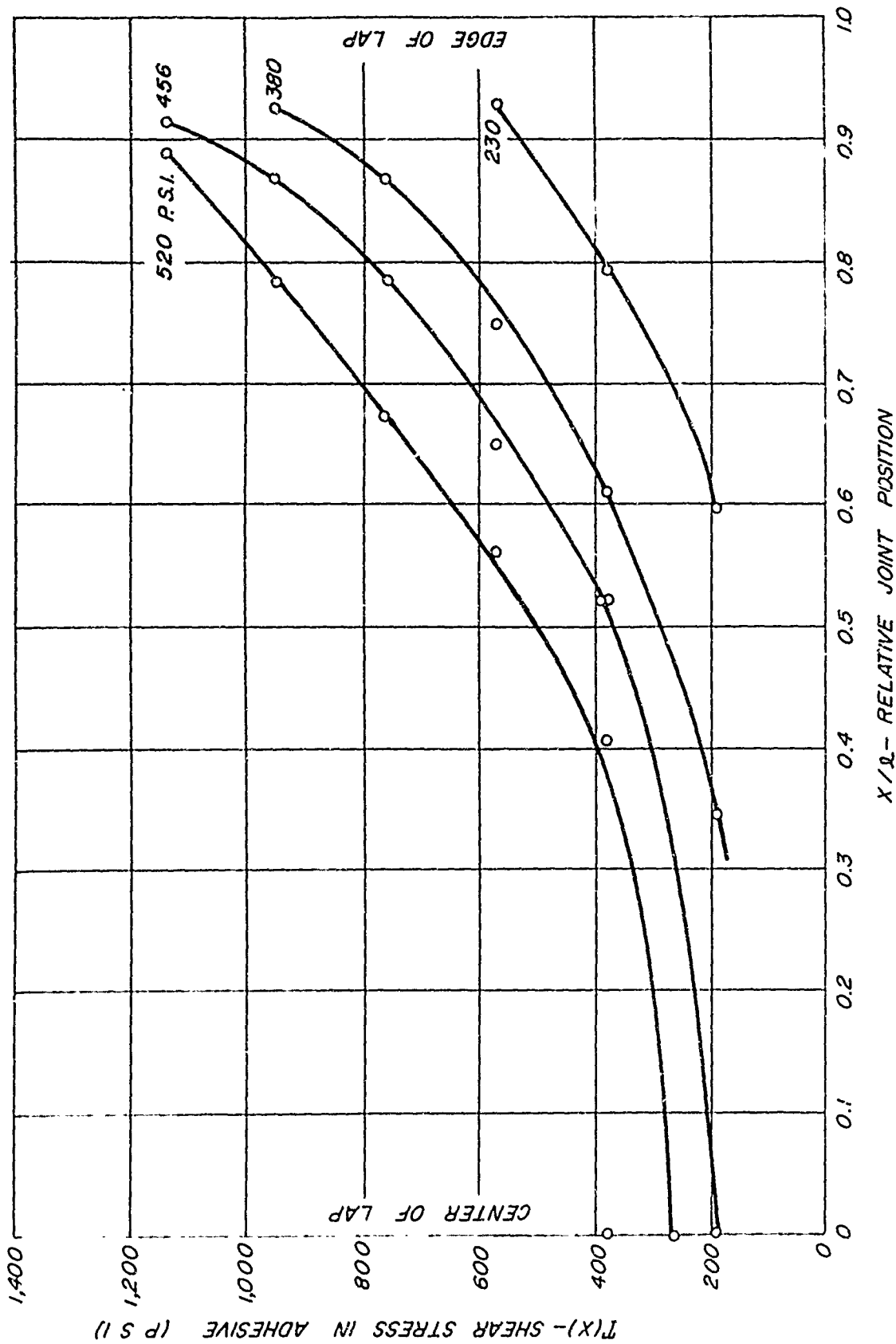


Figure 12.--Shear stress distribution as a function of average shear stress that was experimentally determined for the specimen that had a 0.75-inch overlap. $l = L/2$

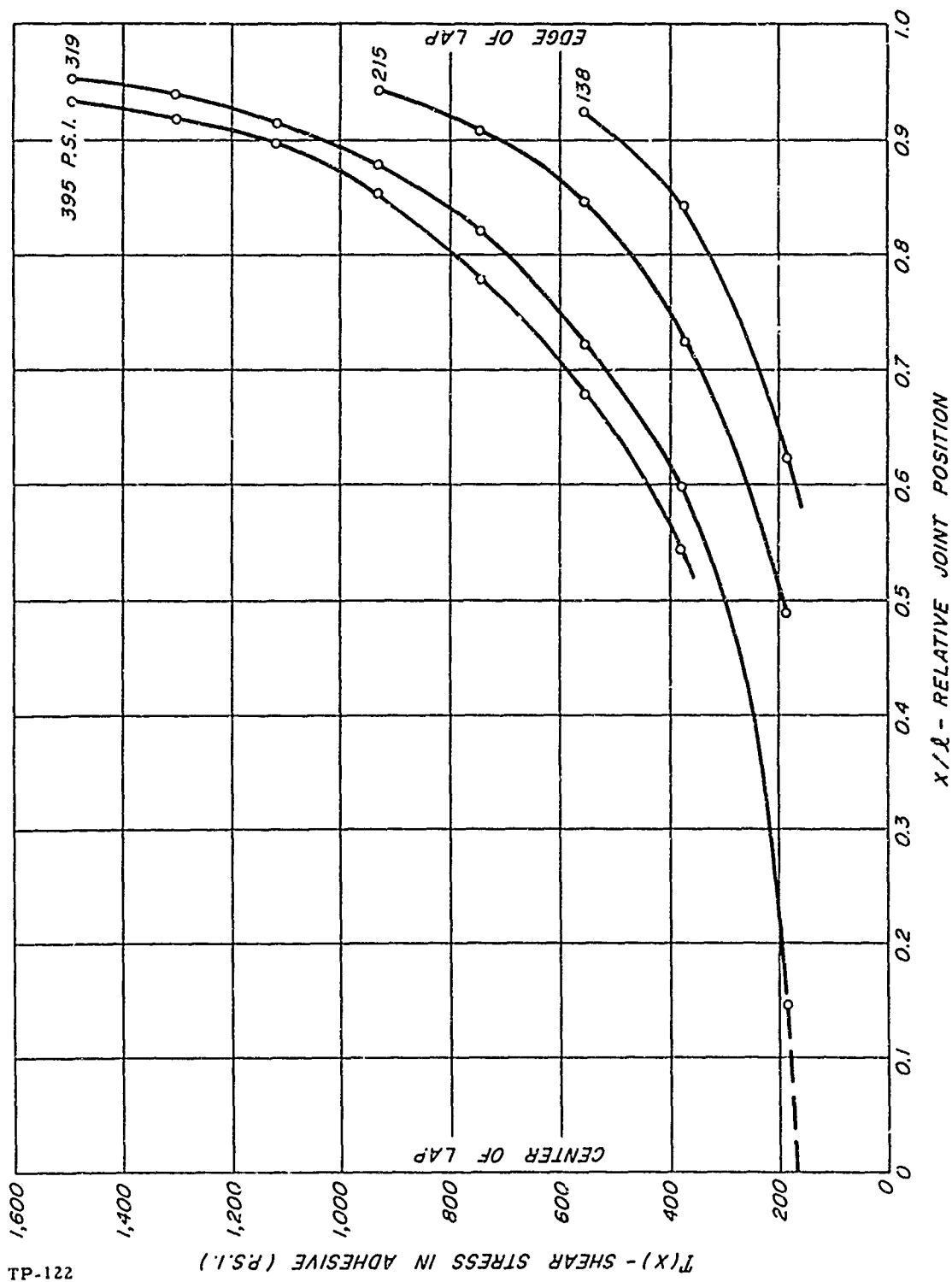


Figure 13.--Shear stress distribution as a function of average shear stress that was experimentally determined for the specimen that had an overlap of 1.03 inches. $l = L/2$

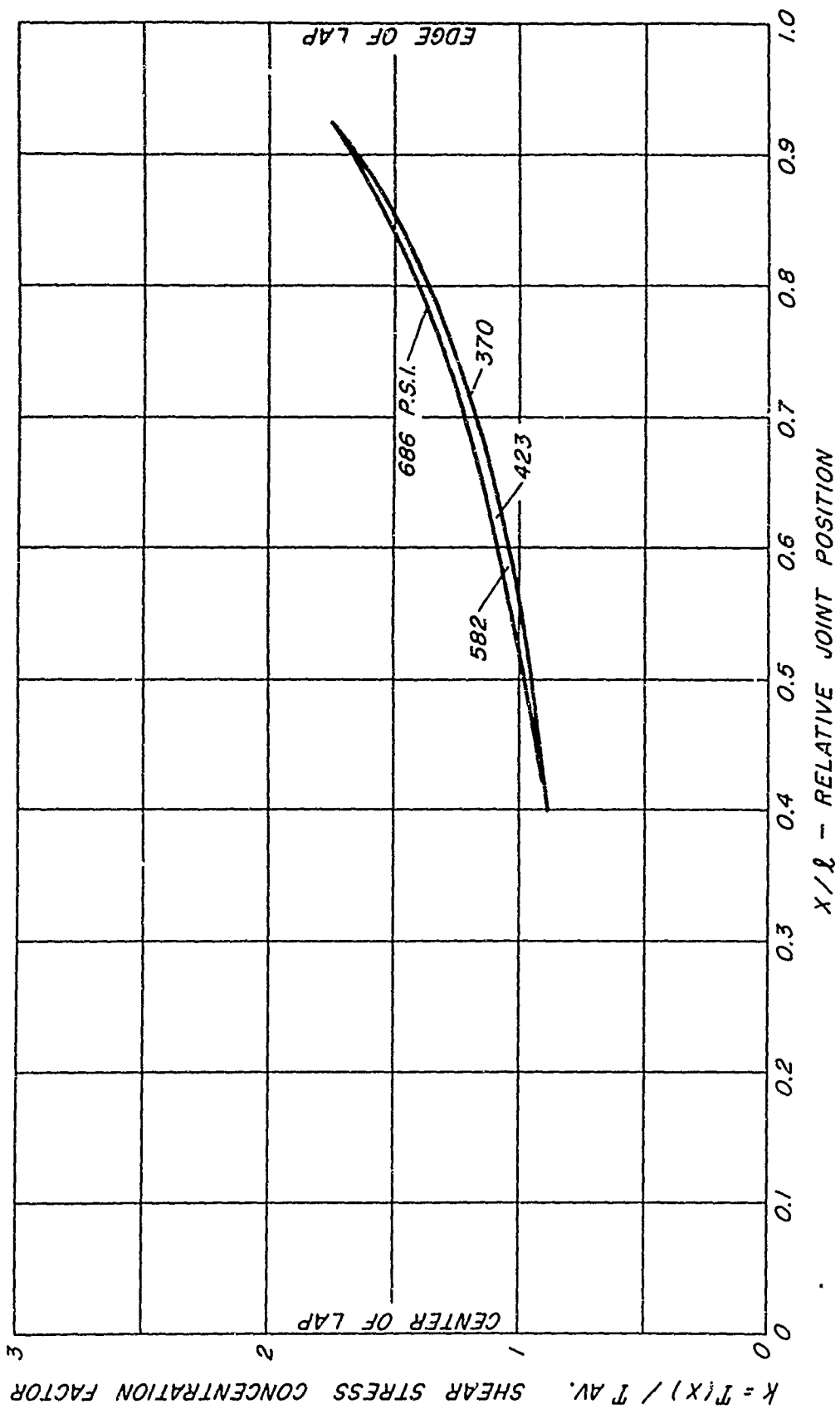


Figure 14.--Distribution of shear stress concentration factor for specimen with 0.35-inch overlap as a function of average shear stress. $l = L/2$

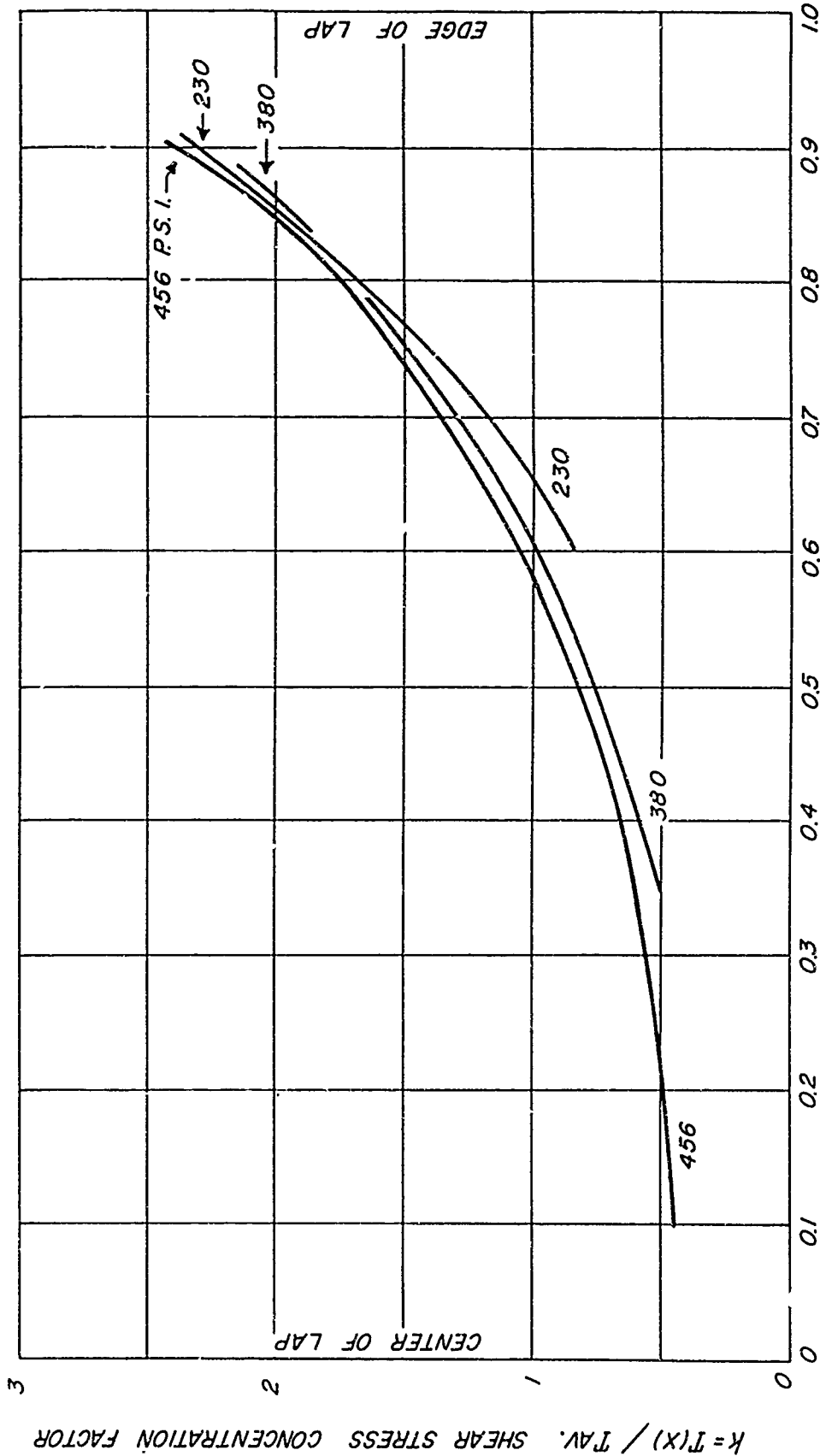


Figure 15. -- Distribution of shear stress concentration factor for specimen with 0.75-inch overlap as a function of average shear stress. $l = L/2$

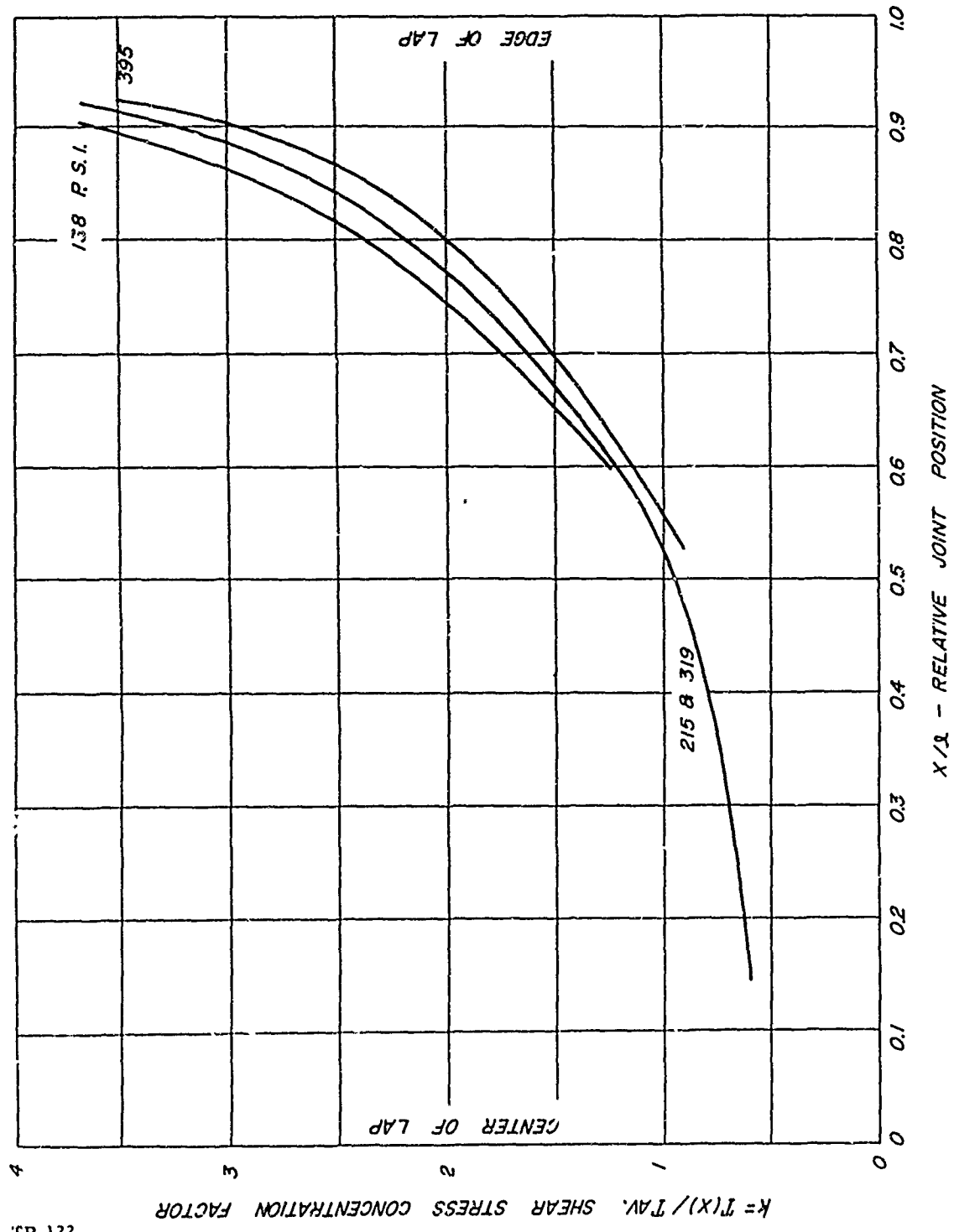


Figure 16.--Distribution of shear stress concentration factor for specimen with overlap of 1.03 inches as a function of average shear stress. $l = L/2$

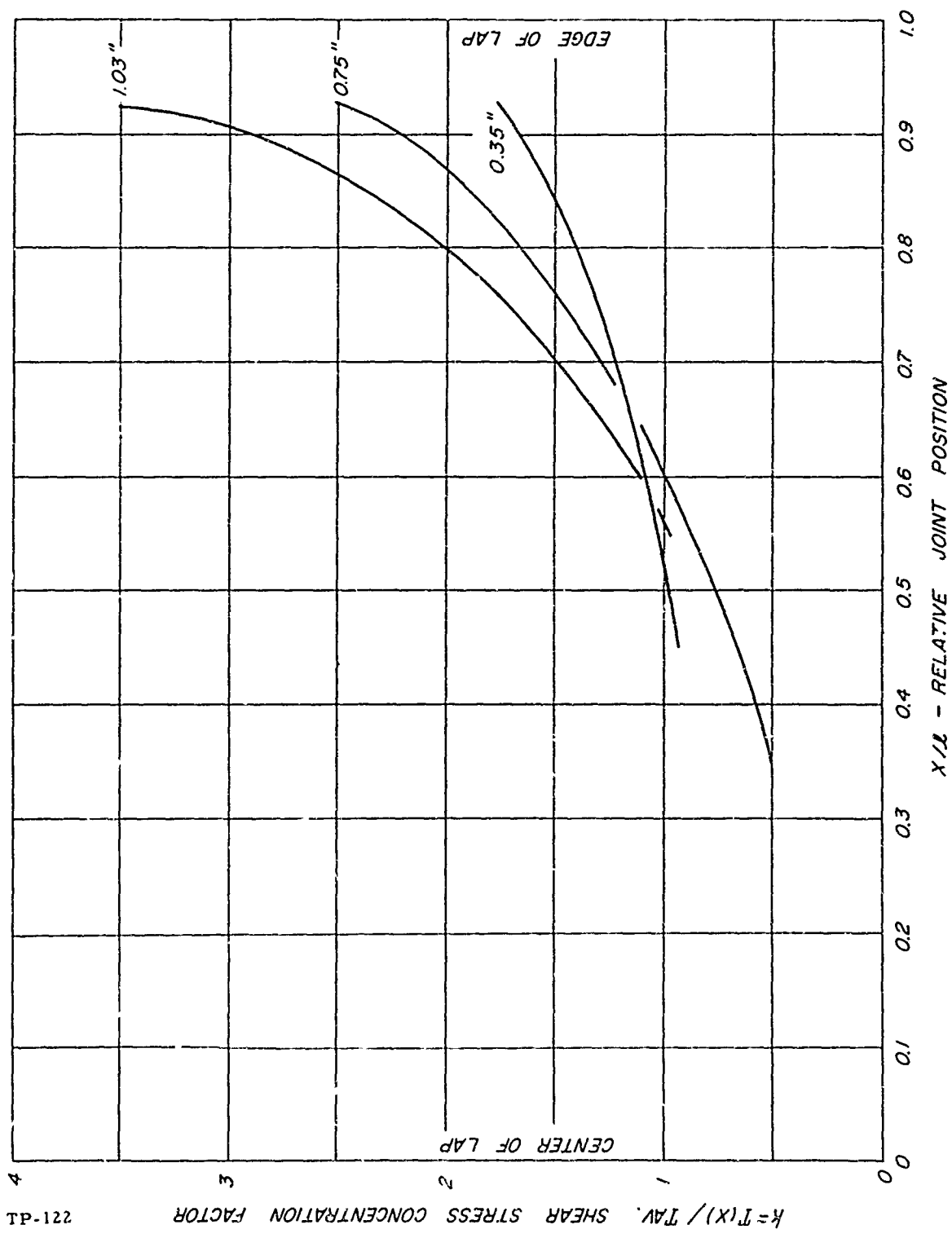
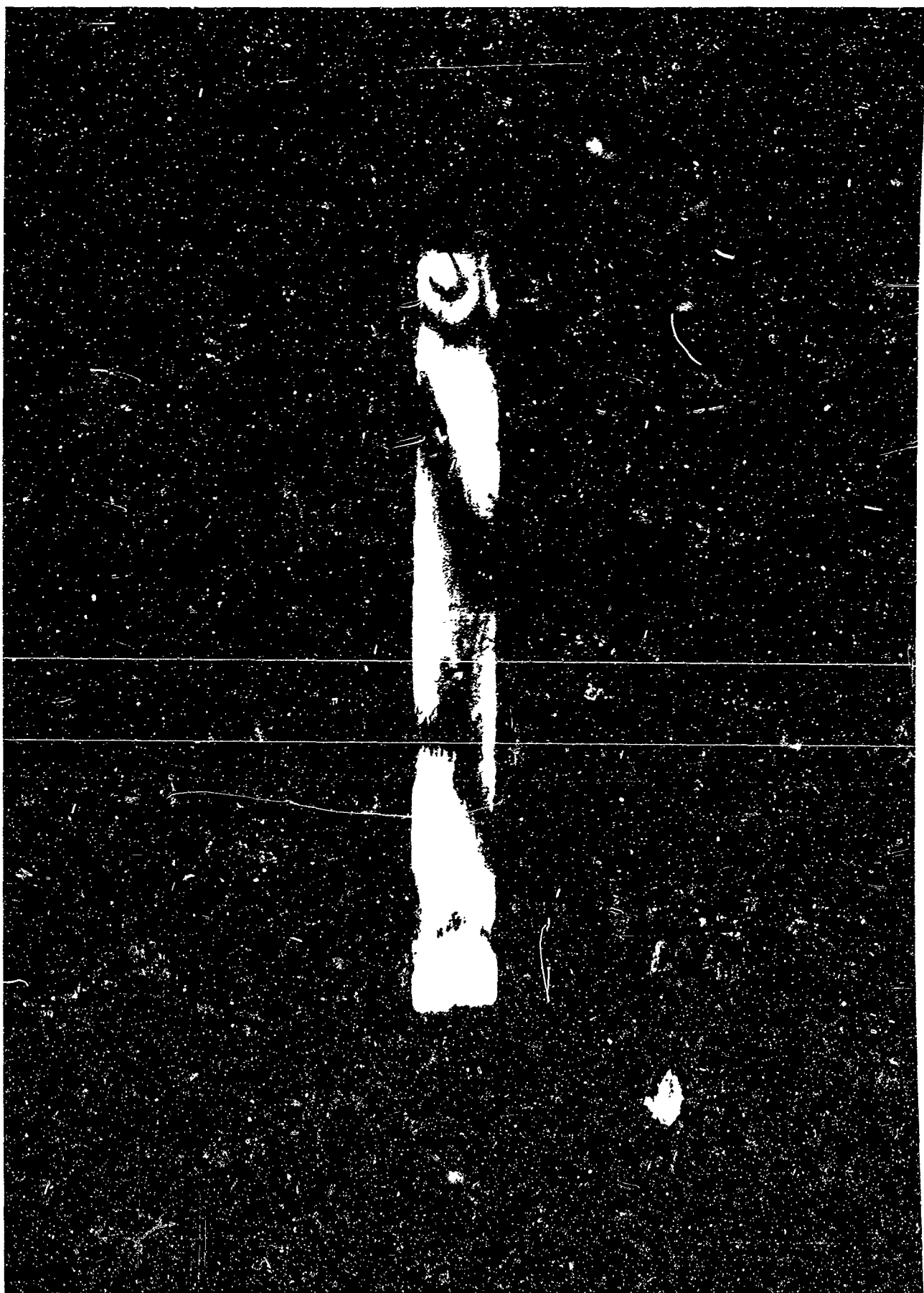


Figure 17.--Distribution of shear stress concentration factor at average shear stress of 370 pounds per square inch as a function of length of overlap.
 $l = L/2$

Figure 18.--Shear stress distribution across the adhesive
film of the specimen that had a 0.28-inch overlap.
Average shear stress was 684 pounds per square inch.

(M 121 566)



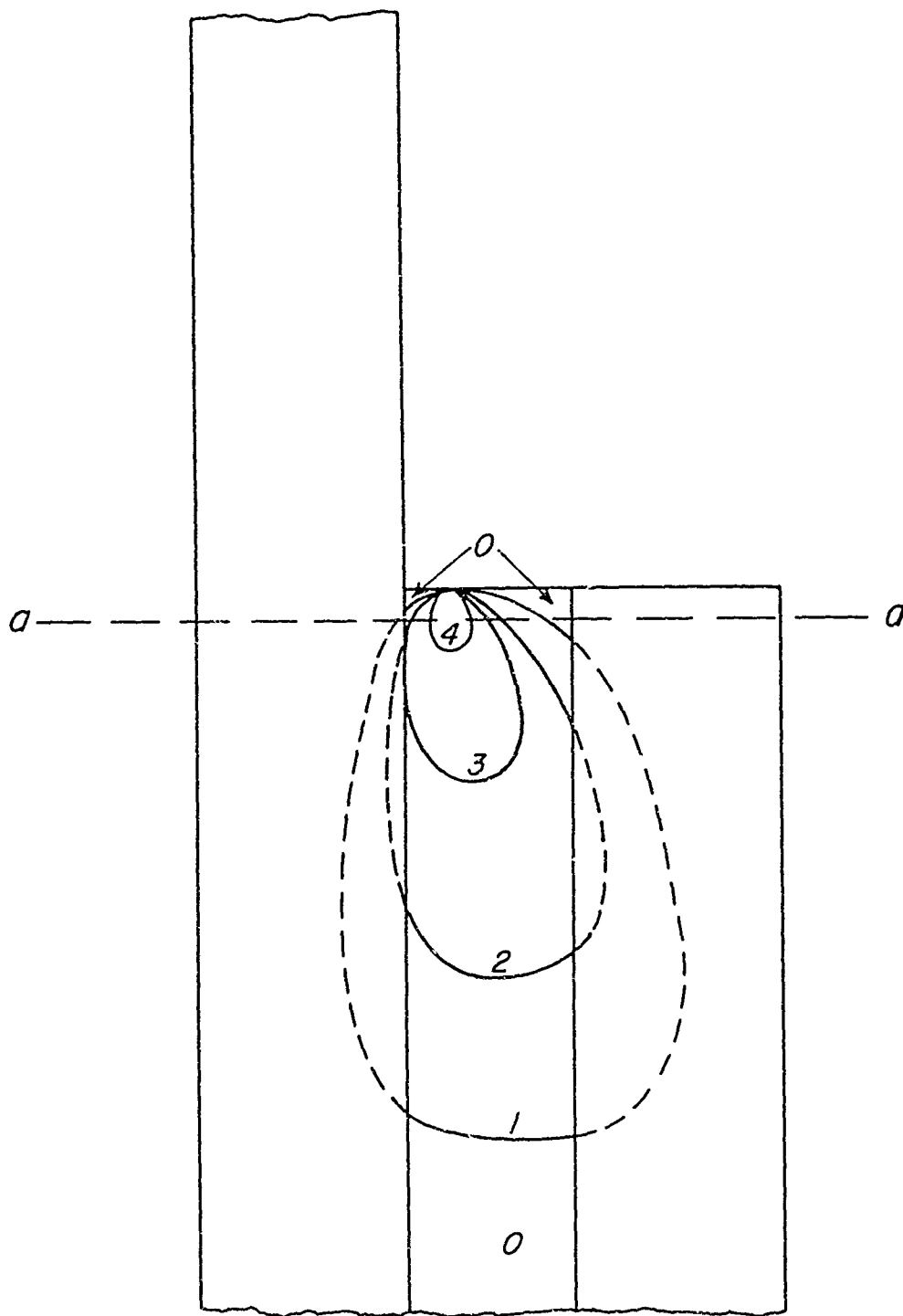


Figure 19.--Schematic interpretation of the fringe pattern development of the specimen with a 0.28-inch overlap.

TP-122

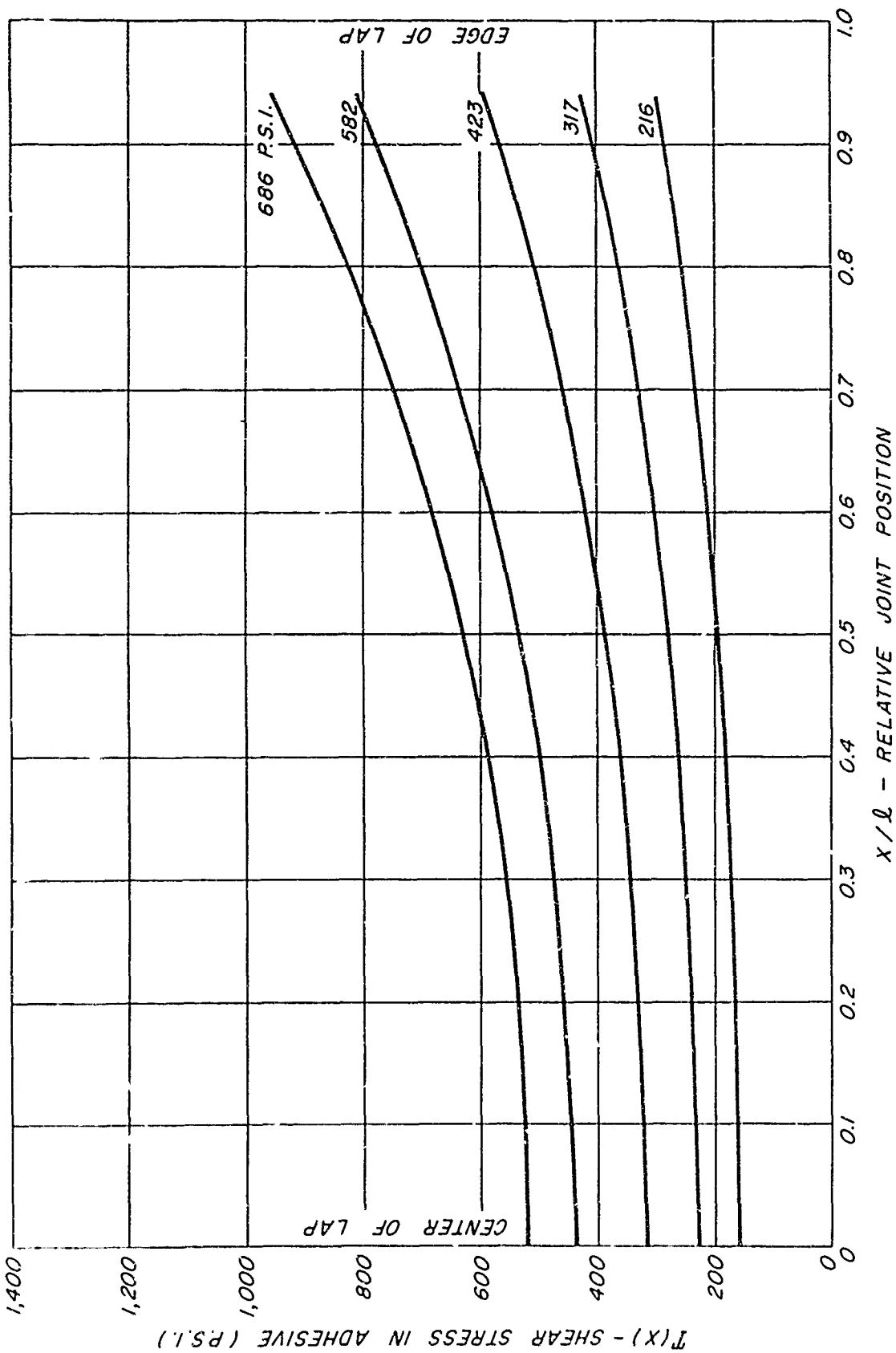


Figure 20. --Theoretical shear stress distribution calculated using Goland and Reissner analysis for the 0.35-inch-overlap specimen as a function of average shear stress. $t = L/2$

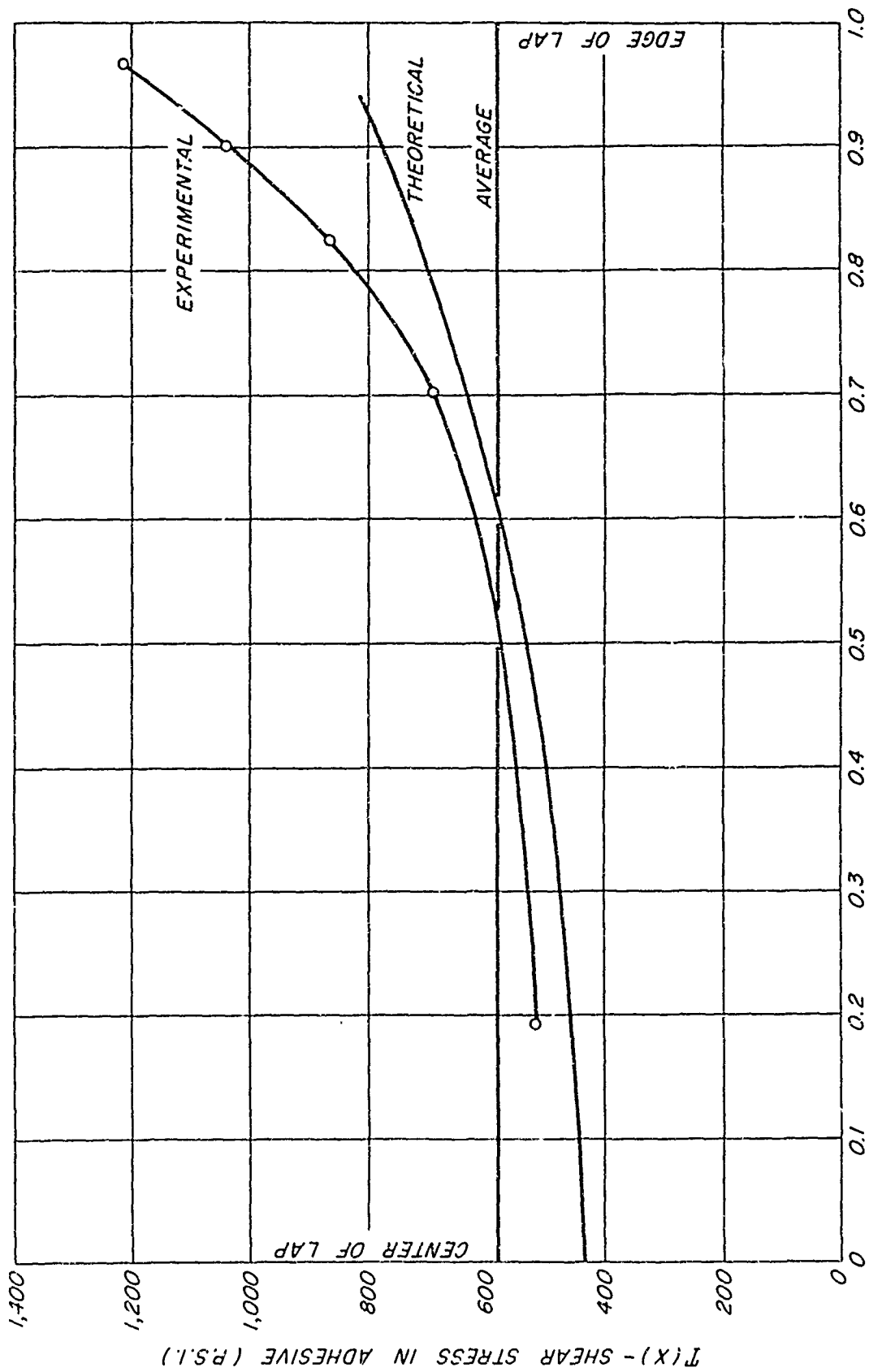


Figure 21. -- Comparison of the theoretical and experimental shear stress distribution at an average shear stress of 582 pounds per square inch for 0.35-inch-overlap specimen. $t = L/2$

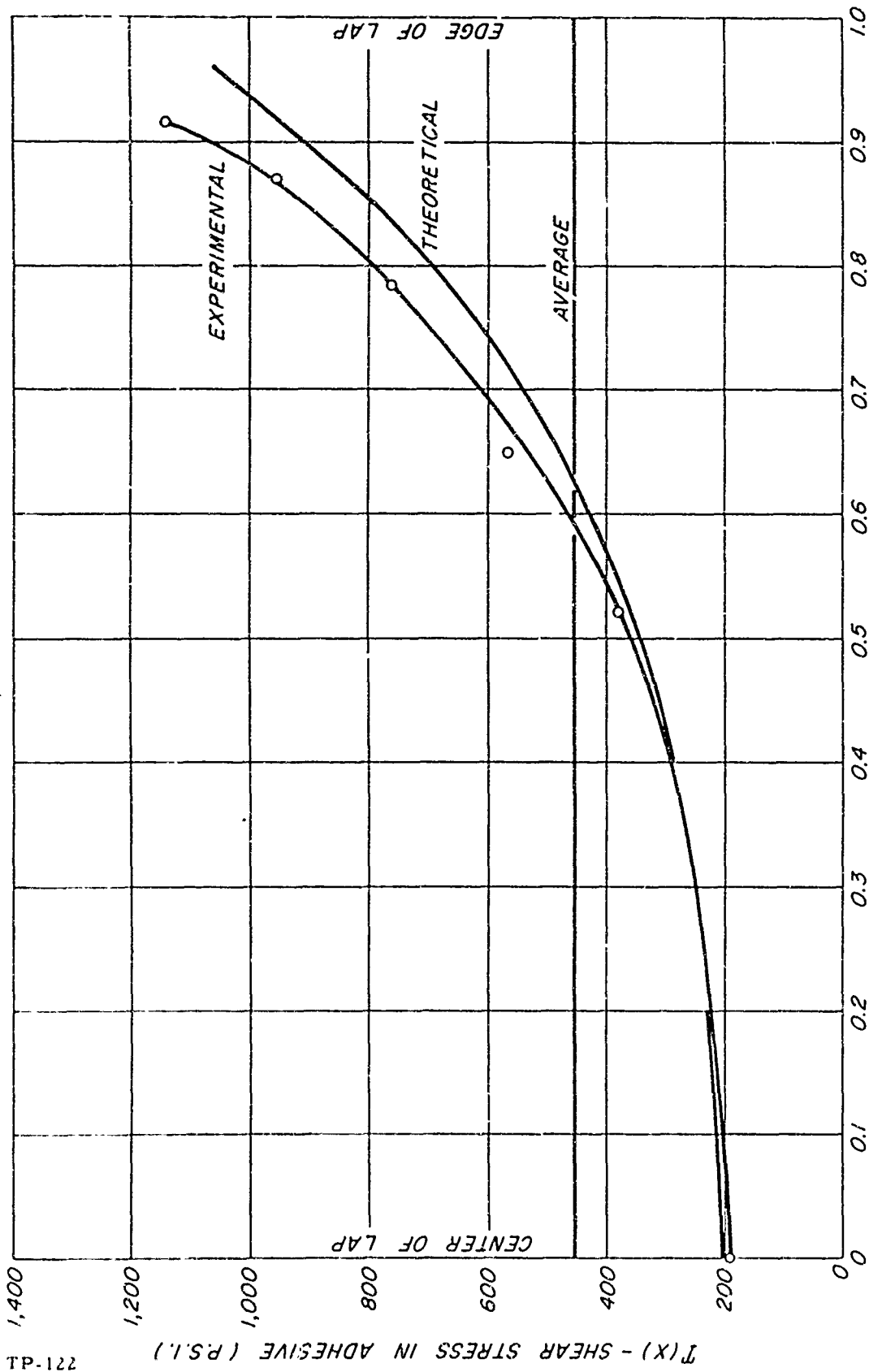


Figure 22. --Comparison of the theoretical and experimental shear stress distribution at an average shear stress of 456 pounds per square inch for 0.75-inch-overlap specimen. $l = L/2$

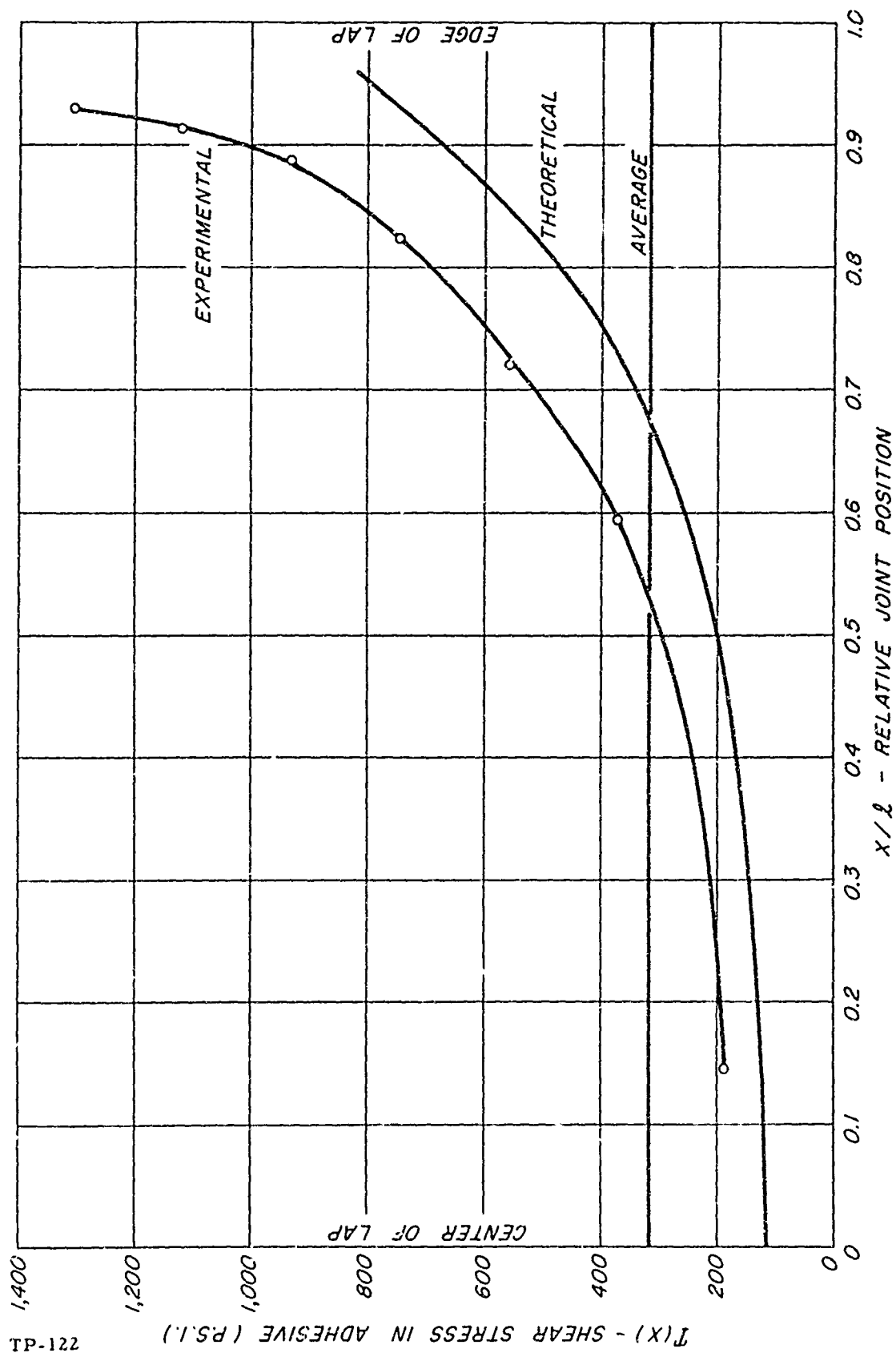


Figure 23. ---Comparison of the theoretical and experimental shear stress distribution at an average shear stress of 319 pounds per square inch for the specimen that had an overlap of 1.03 inches. $l = L/2$

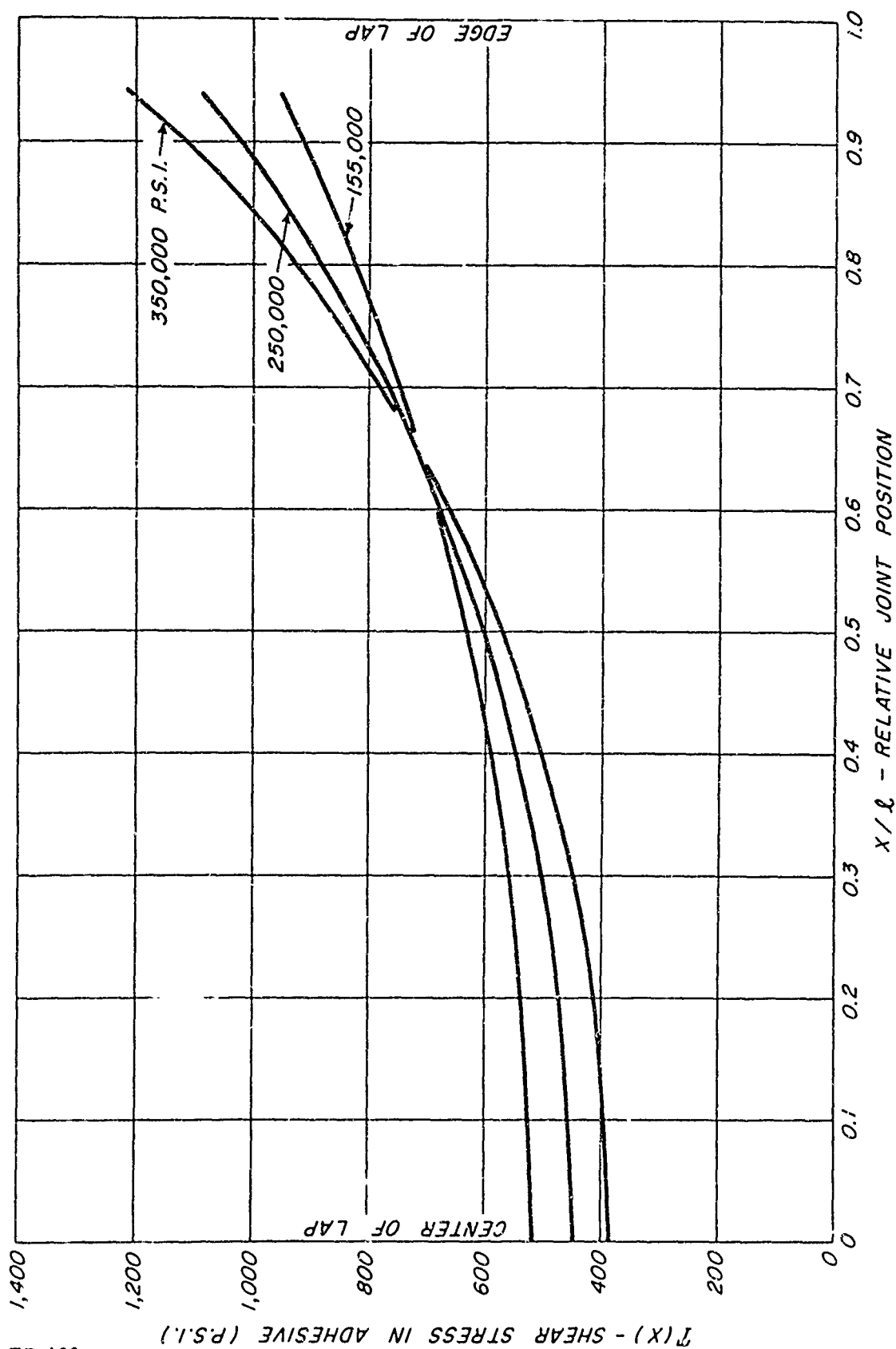


Figure 24. --Theoretical shear stress distribution calculated from Goland and Reissner analysis for the 0.35-inch-overlap specimen at an average shear stress of 686 pounds per square inch as a function of adhesive modulus of rigidity. $l = L/2$